Desalination 532 (2022) 115744

Contents lists available at ScienceDirect

Desalination

journal homepage: www.elsevier.com/locate/desal

A review on state-of-the-art applications of data-driven methods in desalination systems

Pooria Behnam [a], Meysam Faegh [b], Mehdi Khiadani [a,*]

[a] School of Engineering, Edith Cowan University, 270 Joondalup Drive, Joondalup, Perth, WA 6027, Australia
[b] Department of Mechanical Engineering, Sharif University of Technology, Tehran, Iran

HIGHLIGHTS

- Data-driven methods in both membrane and thermal desalination systems are reviewed.
- A variety of AI and DOE methods are used in desalination area are analyzed.
- Applications of different methods in various desalination systems are categorized.
- Influential parameters for different methods and desalination systems are reported.
- Research gaps in terms of desalination systems and data-driven models are proposed.

ARTICLE INFO

Keywords:
Desalination
Data-driven methods
Artificial intelligence
Machine learning
Design of experiment

ABSTRACT

The substitution of conventional mathematical models with fast and accurate modeling tools can result in the further development of desalination technologies and tackling the need for freshwater. Due to the great capability of data-driven methods in analyzing complex systems, several attempts have been made to study various desalination systems using data-driven approaches. In this state-of-the-art review, the application of various artificial intelligence and design of experiment data-driven methods for analyzing different desalination technologies have been thoroughly investigated. According to the applications of data-driven methods in the field of desalination, the reviewed investigations are classified into five categories namely performance prediction using operational parameters, performance prediction using design parameters, optimization and correlation development, maintenance, and control of desalination systems. For each category, valuable information about the data-driven methods such as inputs, outputs, hyper-parameter tuning methods, and size of datasets have been provided and the main remarks are reported. The findings showed that data-driven methods can play a vital role in each aforementioned application for both thermal and membrane-based desalination technologies. Eventually,

Abbreviations: AD, Adsorption desalination; AEO, Artificial ecosystem-based optimization algorithm; AGMD, Air gap membrane distillation; AI, Artificial intelligence; ANFIS, Adaptive neuro fuzzy inference system; ANN, Artificial neural network; ANOVA, Analysis of variance; ARIMA, Autoregressive integrated moving average; BAMLR, Bootstrap aggregated multiple linear regressions; BANN, Bootstrap aggregated neural networks; BBD, Box–Behnken design; BFGS, Broyden–-Fletcher–Goldfarb–Shanno; CCD, Central composite design; CDI, Capacitive deionization; CFD, Computational fluid dynamics; CGF, Conjugate gradient Fletcher reeves update; CGP, Conjugate gradient Powell-Beale restarts; CNN, Conventional neural network; COP, Coefficient of performance; DCMD, Direct contact membrane distillation; DL, Deep learning; DOE, Design of experiment; DRL, Deep reinforcement learning; DT, Decision tree; ED, Electrodialysis desalination; ENN, Elman neural network; FCCD, Face-centered central composite; FD, Factorial design; FO, Forward osmosis; GA, Genetic algorithm; HDH, Humidification-dehumidification; HHO, Harris hawks optimizer; ICA, Imperialist competition algorithm; LM, Levenberg Marquardt; LSTM, Long short-term memory; MD, Membrane distillation; MF, Membership function; ML, Machine learning; MLPANN, Multi-layer perceptron artificial neural network; MSF, Multistage stage flash distillation; NARX, Nonlinear autoregressive exogenous; NSGA, Non-dominated sorting genetic algorithm; OLS, Orthogonal least squares; OSS, One step secant; PGMD, Permeate gap membrane distillation; PSO, Particle Swarm Optimization; QRCD, Quadratic rotation-orthogonal composite design; R^2, Coefficient of determination; RB, Resilient back-propagation; RBFANN, Radial basis function artificial neural network; RF, Random forest; RM, Regression model; RNN, Recurrent neural networks; RO, Reverse osmosis; RSM, response surface methodology; RVFL, Random vector functional link network; SCP, Specific cooling power; SDS, Sodium dodecyl sulfate; SDWP, Specific daily water production; SS, Solar still; SVM, Support vector machine; SVR, Support vector regression; SCG, Scaled conjugate gradient; TDS, Total dissolved solids; TM, Taguchi method; VHD, Vacuum humidification dehumidification; VMD, Vacuum membrane distillation.

* Corresponding author.
E-mail address: m.khiadani@ecu.edu.au (M. Khiadani).

https://doi.org/10.1016/j.desal.2022.115744
Received 30 November 2021; Received in revised form 6 March 2022; Accepted 29 March 2022
Available online 6 April 2022
0011-9164/

the research gaps are highlighted and a roadmap is also provided for future data-driven analysis of various desalination systems and their further advancement.

1. Introduction

It is anticipated that by the year 2050, the water shortage problem turns out to be a serious problem and around 5.7 billion people will face the water shortage [1]. Climate changes, industrialization, and population growth are mentioned as main contributors to this worldwide issue [2,3]. Herein, desalination technologies have started to play a vital role in mitigating water scarcity mainly due to the fact that around 97% of available water on earth are found to be saline and brackish [4].

The employment of accurate and fast analytical tools can lead to significant performance improvement and cost reduction of desalination systems, paving the way for further development of desalination systems and alleviating the water scarcity crisis. However, existing conventional mathematical methods mainly suffer from insufficient accuracy and high complexity due to simplified assumptions employed in their development, the existence of several affecting parameters, and complex phenomena inside the desalination systems [5,6]. In this situation, data-driven methods as robust black-box analytical tools can result in a more precise analysis of various desalination technologies and therefore mitigate the mentioned issues. These methods do not require specific in-depth knowledge about the desalination systems and are generally based on the analysis of a set of input/output data [7].

The great benefits of data-driven methods over conventional mathematical modeling tools have drawn researchers' attention to the use of these promising methods in desalination systems. A number of researchers reviewed the application of classical artificial neural networks (ANN) in membrane-based desalination systems [7–10]. Also, a recent review article has been conducted on the utilization of machine learning (ML) models for performance modeling of solar still desalination systems [11]. To the best of the authors' knowledge, there is a deficiency for a comprehensive review on the application of various data-driven methods including design of experiment (DOE) and artificial intelligence (AI) methods in both thermal and filtration-based desalination systems. Furthermore, the application of data-driven methods for various purposes including the distribution of applied data-driven methods in each desalination system, and the size of data sets have been given insufficient attention in published review studies. Therefore, this study aims to comprehensively discuss and categorize the state-of-the-art publications based on the application of data-driven methods in desalination systems across five categories, including performance prediction using operational parameters, performance prediction considering design parameters, optimization and correlation development, maintenance, and control (Fig. 1). Moreover, the available literature are systematically reviewed and summarized to identify the potential research gaps on the application of data-driven techniques in the desalination area.

2. Overview of desalination technologies and data-driven methods

2.1. Overview of desalination technologies

As shown in Fig. 2, desalination technologies investigated by data-driven tools mainly fall under two categories of filtration-based and thermal processes. The number against each technology represents the data-driven studies that have been conducted to analyze the mentioned desalination technologies and have been reported in the current review. In the case of filtration-based processes, semipermeable membranes are utilized for freshwater production, except for the capacitive deionization (CDI) desalination method in which mainly the porous electrodes are used for salt removal. Furthermore, in the thermal-based process freshwater is mainly produced by vaporization and condensation. A brief description of desalination technologies reviewed in this review paper is provided in Table 1. Readers are referred to cited references for

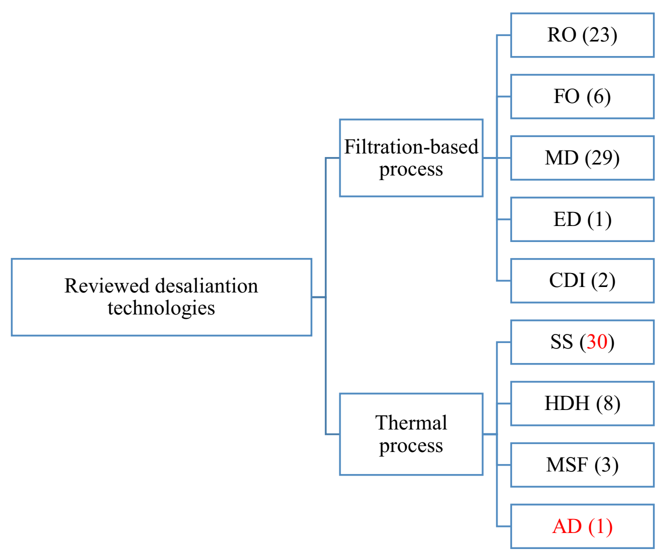

Fig. 2. Desalination technologies analyzed using data-driven methods.

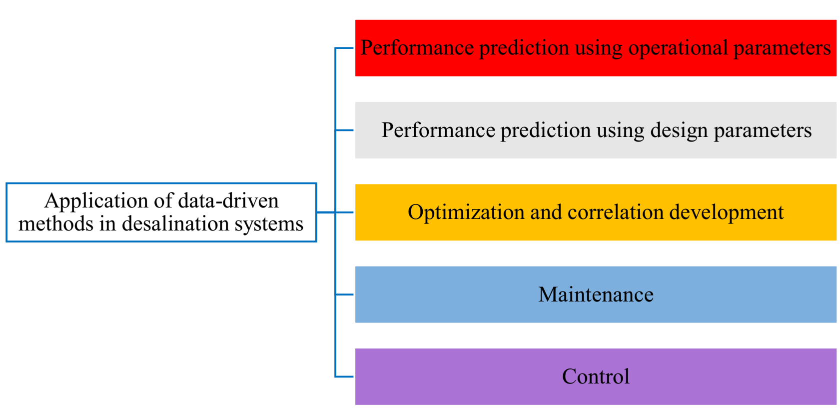

Fig. 1. Applications of data-driven methods in desalination systems.

a more in-depth knowledge about the principle of each desalination technology.

2.2. Overview of data-driven methods

The data-driven methods employed for the analysis of desalination systems can be divided into AI and DOE methods as shown in Fig. 3. AI techniques are capable of estimating the relationship between inputs and outputs without a need for accurate knowledge about the system and therefore are considered as black-box analytical methods [30,31]. Generally, an experimental dataset is employed for developing the AI techniques where the whole dataset is divided into two or three parts

Table 1
A brief description of reviewed desalination systems.

Ref	Desalination technology	Type	Driving force	Key influential parameters	Main remarks
[12–14]	Reverse osmosis (RO)	Filtration	Pressure gradient	• Feed pressure • Feed temperature • Salt concentration of feed flow • Membrane characteristics	• RO is a water purification process driven by pressure to overcome osmotic pressure for producing freshwater with the aid of a partially permeable membrane. • Although the RO method is an energy-intensive desalination process, this technology is the most dominant desalination process worldwide due to its high efficiency and comparatively low water cost.
[5,15,16]	Forward osmosis (FO)	Filtration	Osmosis pressure	• Temperature of draw solution • Osmotic pressure difference • Feed solution velocity • Draw solution velocity • Membrane properties	• FO utilizes the natural energy of osmotic pressure to separate water from dissolved solutes via a semi-permeable membrane. The osmotic pressure is used to transport water through the membrane while retaining all the dissolved solutes on the other side. • Concentration polarization and fouling are two main issues of the FO process.
[17,18]	Membrane distillation (MD)	Filtration	Vapor pressure gradient	• Feed flow temperature • Mass flow rates • Module geometric parameters • Membrane properties	• MD process is a hybrid membrane/thermal process that permits only water vapor to permeate through the membrane due to the hydrophobic characteristics of its membrane. • Based on the method of water vapor collection, MD modules are divided into 4 main categories: direct contact membrane distillation (DCMD), air-gap membrane distillation (AGMD), vacuum membrane distillation (VMD) and sweep gas membrane distillation (SGMD) • Wetting/fouling of membrane and temperature/concentration polarizations are the main issues of MD desalination processes. • The required energy can be effectively supplied by solar energy.
[19,20]	Electrodialysis desalination (ED)	Filtration	Electrical potential gradient	• Temperature and flow rate of feed flow • Applied voltage • Initial feed composition • Membrane characteristics	• ED is a low-pressure process that uses ion-selective membranes to desalinate water. ED deploys charged membranes and uses electrical energy to flow the ions against a concentration gradient causing separation and purification. • Membrane fouling is a serious obstacle to scaling up the ED technology. • Solar/wind energies can be integrated well with the ED technology.
[21]	CDI	Filtration	Electrical potential gradient	• Electrode materials • Salt concentration • Electrode specific surface area	• CDI process uses the electrical potential difference applied over two electrodes to deionize the water. • The CDI process comprises two main cell architectures: static electrode architecture and flow electrode architecture. • Anion/cation exchange membranes are added for performance enhancement. • The CDI technology is still on the laboratory scale.
[22]	Solar still (SS)	Thermal	Heat	• Solar intensity • Water depth	• Solar still utilizes direct solar radiation to desalinate saline water based on the evaporation and condensation process. • Solar still is mainly fallen into active and passive categories. • Despite low efficiency/freshwater productivity, the solar still technology is simple and suitable for remote areas.
[23–25]	Humidification-dehumidification (HDH)	Thermal	Heat	• Mass flow ratio of water to air • Top temperature of the cycle • Packing materials	• HDH is a desalination technology that imitates nature's rain cycle. In the humidifier, water is sprayed into the air and then, it condenses to freshwater by passing through the dehumidifier. • There are several configurations based on the heated fluid (water-heated and/or air-heated) and the type of fluid circulation (open or close cycles) • Low-temperature heat sources such as solar energy and waste heat can be utilized in HDH desalination systems.
[26,27]	Multistage stage flash (MSF) distillation	Thermal	Heat	• Top brine temperature • Number of stages • Temperature drop in each stage • Brine temperatures at inlets and outlets	• In the MSF process, feed seawater is pressurized, heated and discharged to a chamber with slightly lower water saturation vapor pressure. Next, a fraction of this water flashes into steam and condenses on the exterior surface of heat transfer tubing. • The temperature of each stage is kept under the saturation temperature of the water entering each stage and vacuum pressure is mainly applied to this end. • Evaporation temperature decreases from the first stage to the last one using changing the vacuum pressures. • Top brine temperature is in the range of 80 °C to 125 °C.
[28,29]	Adsorption desalination (AD)	Thermal	Heat	• Heat source temperature • Preheating time • Adsorption/desorption time • Heat recovery time	• Adsorption desalination system has the capability of providing both freshwater and cooling effect simultaneously. • AD is a promising method to run with solar and waste energies. • Main performance indicators of the AD system are coefficient of performance (COP), specific cooling power (SCP), and specific daily water production (SDWP).

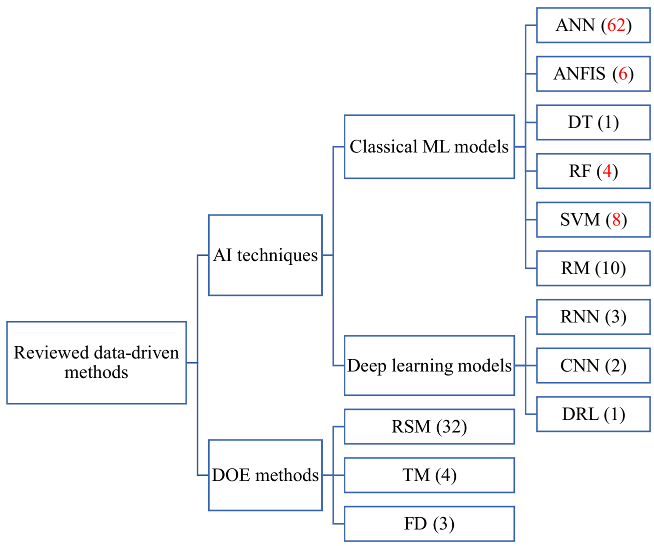

Fig. 3. Classification of data-driven methods applied in desalination area.

namely training, (validation), and testing sub-datasets. The training dataset consists of a larger number of data to train the AI model, while validation and testing datasets are unseen datasets comprised of a lower number of data that are mainly used to estimate the accuracy and generalization power of the developed AI methods. The predictive performance of AI models is highly dependent on a number of key factors including the accurate selection of inputs and outputs, hyper-parameter tuning methods, and size of datasets [32]. As shown in Fig. 3, AI techniques can be classified into classical ML and deep learning (DL) methods. The classical ML methods employed for studying desalination systems consist of Artificial neural network (ANN), Adaptive neuro fuzzy inference systems (ANFIS), Decision tree (DT), Random forest (RF), Support vector machine (SVM), and Regression models (RM). Furthermore, DL methods have more complex structures compared to classical ML methods and mainly require a larger number of data. The great benefits of DL models over the classical ML methods such as favorable capability in the analysis of unstructured data (such as photos) and great ability for analyzing the dynamic systems have recently captured the researchers' attention working on desalination area [33,34]. DL methods applied in desalination systems can be categorized into three methods namely recurrent neural networks (RNN), conventional neural network (CNN), and deep reinforcement learning (DRL).

DOE method is mainly derived from statistical methods and was initially proposed by Fisher in the 1930s for the research in agricultural and biological domains [35]. Compared to the conventional one-factor-at-a-time experimental method, the DOE approach can significantly lower the cost and time of the data-acquisition process while providing the maximum information about the system behavior by wisely designing the required experimental tests. Moreover, the DOE approach takes into account the interaction effects of independent variables on system behavior and can be effectively applied for performance prediction and optimization purposes. Response surface methodology (RSM), Taguchi method (TM), and factorial design (FD) are the three main statistical DOE tools that have been widely used to analyze the performance and optimization of desalination systems. It is also worth mentioning that the number of reviewed studies for each data-driven model is reported in Fig. 3. Moreover, a brief description of AI and DOE methods is summarized in Table 2 and the readers are referred to corresponding references for more detailed information about each data-driven method.

Table 2
A brief description of applied data-driven methods in desalination systems.

Ref	Method	Type	Main remarks
[36–41]	ANN	ML	• ANNs are comprised of several neurons which mimic the brain data processing approach. Each neuron has several inputs from other neurons corresponding to their weights and employs a non-linear activation function to produce the output signal which may transfer to other neurons. • Several activation functions have been used in ANNs such as sigmoid, Gaussian radial basis function, hyperbolic tangent, etc. • Different types of ANN models have been employed to study desalination systems including multi-layer perceptron artificial neural network (MLPANN), radial basis function artificial neural network (RBFANN), bootstrap aggregated neural networks (BANN), nonlinear Autoregressive Exogenous (NARX), Elman neural network (ENN), and random vector functional link network (RVFL) • The developed ANN models in the field of desalination have used different training algorithms including Levenberg Marquardt (LM) [42], Imperialist competition algorithm (ICA) [43], genetic algorithm (GA) [44], one step secant (OSS) algorithm [45], conjugate gradient Powell-Beale restarts (CGP) [46], scaled conjugate gradient (SCG) [46], resilient backpropagation (RB) [47], gradient descent algorithm [48], Broyden–Fletcher–Goldfarb–Shanno algorithm (BFGS) [49], and Bayesian optimization method [50]. • Type of activation function, number of hidden layers, and number of neurons in hidden layers are three main hyper-parameters which optimized via trial and error method or optimization techniques.
[51]	ANFIS	ML	• ANFIS model is a combination of ANN and Takagi-Sugeno fuzzy systems which is benefited from the learning capability of the ANN model and the reasoning ability of the fuzzy system. • ANFIS is mainly a 5-layer network comprised of five layers namely fuzzification, product, normalization, defuzzification, and output layers. • Different membership functions can be used such as Pi-shaped, sigmoidal, triangular-shaped and trapezoidal-shaped. • Grid partitioning and clustering methods are used to generate the fuzzy system. • Hyper-parameters include types of membership functions and the number of clusters.
[32,52]	DT	ML	• DT is a supervised ML method that uses if-then-else decision rules to predict the target. • The data split process begins from the top node of the tree called the "root node" and ends up at leaf nodes. • Data is split at each node appropriately considering the best input feature and corresponding threshold which leads to the lowest error. • DT method does not require input normalizations before developing the tree. • DT is highly vulnerable to overfitting and needs accurate hyper-parameter tuning. • The maximum depth of the tree, the minimum number of samples required for splitting, and the number of maximum features are the three main hyper-parameters for the DT model.
[52,53]	RF	ML	• RF model is an ensemble of trees and the averaging method is used to predict the final target. • Each tree in the forest is created by a subset of training dataset called "bootstrapped dataset". A random subset of features is also selected to build the trees.

(*continued on next page*)

Table 2 (*continued*)

Ref	Method	Type	Main remarks
			• The applied randomness in developing the forest results in a better generalization capability in comparison with the DT model. • There is no need for the input normalization process prior to training the RF model. • RF method can inherently determine the most influential inputs. • Four hyper-parameters exist in the RF model: The maximum depth of the tree, the minimum number of samples required for splitting, the number of maximum features, and the number of trees.
[32,52]	SVM	ML	• The development of SVM model is based on a subset of the training dataset and the cost of close predictions to their targets is neglected, resulting in training the SVM model even with a small-sized training dataset. • The radial basis kernel function is often used to add non-linearity and mapping data to the feature space. • The SVM regression method needs tuning four hyper-parameters including the type of kernel function, kernel coefficient, penalty parameter, and radius.
[54,55]	RM	ML	• Linear RMs include simple linear regression models, multiple-linear regression models, and step-wise regression models. • Multiple-linear RM considers the effects of multiple independent variables on a dependent variable. • Step-wise RM follows an iterative procedure in which independent variables and coefficients are appropriately selected to develop the linear RM method.
[56]	RNN	DL	• RNN is capable of memorizing the fed inputs and therefore is suitable for analyzing the sequential data and specifically for analyzing the time-related systems. • Long short term memory (LSTM) is a type of RNN model which solved the gradient vanishing problem of the RNN model.
[56]	CNN	DL	• CNN model is a kind of ANN model which is composed of several hidden layers including convolutional, fully connected, flatten, normalization and dropout layers. • CNN model is suitable for pattern recognition and image processing applications.
[57]	DRL	DL	• Reinforcement learning utilizes an agent that learns to make appropriate decisions by trial and error. There is a reward for each decision that leads to the best training state. • DRL is a combination of reinforcement learning and DL methods which DL methods are used to assist the agent to reach the goal.
[35,58]	RSM	DOE	• The RSM method is comprised of both mathematical and statistical approaches. • The RSM method establishes a linear or quadratic polynomial function where the least square method is utilized to determine the regression coefficients. • Different designs such as central composite design (CCD), Box-Behnken design (BBD), face-centered central composite design (FCCD), and quadratic rotation-orthogonal composite design (QRCD) are used in the RSM method. • The CCD is the most popular design for developing the quadratic polynomial function.
[59,60]	TM	DOE	• TM method is a fractional factorial design that requires the lowest number of experiments among DOE methods. • Orthogonal array and signal-to-noise ratio are two main tools for applying the TM design. • Orthogonal array is a matrix allowing the selection of subsets of a combination of independent factors at several factors. • Signal-to-noise ratio is defined as the ratio of sensitivity to variability and depending on the objective function should be minimized, nominal, or maximized.
[61,62]	FD	DOE	• FD design is comprised of full factorial design and fractional factorial design. • The full factorial design considers the total possible combinations of inputs and therefore $2^{\text{number of factors (inputs)}}$ experimental test is required. • The fractional factorial design is used to reduce the number of experiments compared to the full factorial design. This design can be applied when the high order interactions among inputs are assumed unimportant. $2^{\text{number of factors (inputs)-number of reduced factors}}$ experimental tests is needed for the fractional factorial design.

3. Applications of data-driven methods in desalination systems

3.1. Performance prediction using operational parameters

Table 3 summarizes the studies that employed data-driven methods to predict the performance of different desalination systems using operational parameters (listed as inputs in Table 3). The details of the data-driven methods, input and output parameters, and main remarks of each study are presented in Table 3. It can be seen that the most of studies were concentrated on RO and SS desalination systems, and only a few investigators have used data-driven methods to predict the performance of MD, MSF and CDI systems. The most important highlights drawn from Table 3 are presented below.

3.1.1. Use of classical ML models

It can be seen from Table 3 that most of the studies used ANNs to predict the performance of various desalination systems [37,63–78]. This lies in the fact that the ANN model has the privilege of performance anticipation of non-linear systems with high generalization capability and accuracy. In addition to ANNs, there are a couple of classical ML models that have been used to predict the performance of various desalination systems. Pascual et al. [79] used support vector regression (SVR) to predict the performance of a RO plant. It was concluded that the SVR model has the capability of predicting the flowrate and conductivity of both permeate and retentate flows, with average absolute relative errors of 0.70%–2.46%. Bahiraei et al. [80] used ANFIS to predict the energy efficiency of a SS system. It was shown that R^2 values for the training and test sets reached 0.9884 and 0.9906, respectively. Also, it was shown that ANFIS can be used to predict the water productivity in SS systems with 99.99% correlation coefficient [81].

3.1.2. Comparison of ML models and conventional methods

Conventional methods like empirical/statistical models, mathematical methods, and thermodynamic analysis are becoming substituted by ML models in different applications including the field of desalination in recent years. Therefore, some researchers aimed at comparing the performance of ML models with conventional methods in performance prediction of various desalination systems. ML models are usually trained and tested with experimental data to assure their predictive performance. It was reported that there was approximately 5% deviation between the predictions by ANN models and the actual experimental data gathered from a SS system [63]. Also, the ANN prediction for SS processes using the experimental dataset showed better results compared to the mathematical modeling [64]. The performance analysis of a heat pump assisted HDH system indicated that the MLPANN outperformed the conventional compressor polynomials method in predicting the heat transfer rates [37]. For a RO system, both ANNMLP and ANNRBF networks outperformed the conventional statistical models [65]. Similarly, it was reported that in MSF desalination plants, RBFANN

Table 3
Summary of studies on the performance prediction of desalination systems using operational parameters.

Ref	Year	System type	Data-driven method	Dataset size	Inputs	Outputs	Main remark
[63]	2020	SS (solar earth still)	MLPANN	48	• Solar radiation • Water, glass and ambient air temperature	• Water productivity	• ANN architecture: 4–10–10-1 • Hyper-parameter tuning method: Trial and error • Data split ratio: train: 70%, validation:15%, and test: 15% • LM method is used for training. • There was approximately a 5% deviation between the predictions by developed models and the actual experimental data.
[64]	2020	SS integrated with solar panels and cylindrical parabolic collectors	MLPANN	256	• Water, glass cover, insulation, ambient air and basin temperature • Solar Intensity • Wind speed	• Water productivity	• ANN architecture: 7-7-1 • Hyper-parameter tuning method: Trial and error • Data split ratio: train: 70%, valid:15%, test: 15% • LM and hyperbolic tangent sigmoid transfer are used for training method and transfer function, respectively. • The ANN prediction was in good agreement with experimental data and also it was more accurate than the mathematical model.
[37]	2021	HDH integrated with a heat pump	ANFIS, MLPANN, RBFANN	180	• Saturation temperature of the evaporator and evaporative condenser • Spraying saline water temperature • Refrigerant and air mass flow rates • Dry-bulb and wet-bulb temperatures of ambient air	• Gain output ratio • Heat transfer rate of the evaporator and evaporative condenser	• MLPANN model showed the best generalization capability compared to ANFIS and RBFANN models. • MLPANN outperformed the conventional compressor polynomials method.
[65]	2015	RO	MLPANN, RBFANN	–	• Temperature • Pressure • pH • Conductivity	• Permeate flowrate • Permeate TDS	• Data split ratio: train: 70%, and test: 30% • Both developed networks were better than the conventional statistical model. • The MLP network had gained better performance when trained by LM algorithm, having the tangent hyperbolic function as the activation function in the hidden layer neurons. • The RBF network is trained using the backpropagation OLS algorithm by considering the Gaussian radial basis function as the activation function in the hidden layer.
[66]	2010	MSF	RBFANN	380	• Boiling point temperature • Salinity	• Temperature elevation	• ANN architecture: 2-12-1 • Data split ratio: train:70%, validation: 15%, and test: 15% • It was mentioned that top brine temperature plays a key role in performance of MSF desalination method and a suitable temperature elevation can control this parameter. • Accurate prediction of temperature elevation can pave the way for lowering the danger of corrosion and energy consumption in the MSF desalination method. • The developed RBFANN model had better predictive performance compared to the MLPANN model, empirical correlations, and thermodynamic models.
[67]	2020	SS with Cu2O–water nanofluid and thermoelectric cooler	MLPANN	48	• Time • Solar radiation • Fan power • Ambient temperature • Glass temperature • Water temperature • Basin temperature • Nanoparticle concentration	• Water productivity	• ANN architecture: 8–6-1 • Hyper-parameter tuning method: trial and error • Data split ratio: train: 80% and test: 20% • ICA and GA were used for training the MLPANN model. • Both GA-MLP and ICA-MLP models showed better predictive performance than common MLP model. Further, ICA-MLP had an enhanced performance compared with GA-MLP model.

(continued on next page)

Table 3 (*continued*)

Ref	Year	System type	Data-driven method	Dataset size	Inputs	Outputs	Main remark
							• The root mean square error decreased 40.49% and 62.01% compared to the MLPANN by using the GA and ICA algorithms, respectively.
[68]	2016	RO	MLPANN	97–129	• Influent concentration • Temperature • Recovery percentage • Influent flow	• Effluent TDS	• A model was developed to simulate eight types of RO membranes. • Levenberg–Marquardt and Tansig are used as training method and transfer function, respectively. • ANN models can be adapted with new data and upgraded with them. • Neurons were varied from 4 to 6 and 8–13 for the first and second hidden layers. • The most important uncertainty would be caused by uncertainty of input data.
[69]	2013	RO	ANN	9	• Silicon oxide inlet concentration • TDS inlet • Time	• Permeate flow	• Data split ratio: train: 33.3%, validation:33.3%, and test: 33.3% • First and second hidden layers were consisted of four and three neurons, respectively. • It was reported that the ANN with fitness approximation network resulted in lowest MSE and the highest determination coefficient.
[70]	2005	RO	ANN	63	• Feed pressure • Temperature • Salt concentration	• Water permeate rate	• Number of neurons in first and second hidden layers: 3,5,10,15
[71]	2020	RO	MLPANN with GA	70	• Inlet flow rate • Inlet pressure • Inlet temperature • Inlet concentration	• Response parameter of chlorophenol rejection	• Data split ratio: train: 68.57%, validation: 15.71%, and test: 15.71% • Model performance was tested by considering 2 and 8 neurons in hidden layers.
[72]	2020	RO	MLPANN	1806	• Plant location • Plant capacity • Project award year • Raw water salinity • Plant type • Project financing type	• Capital cost of the plant	• The proposed model can be used to make a reasonable estimate of investment costs of upcoming RO plant projects.
[73]	2015	SS (single stage)	MLPANN	160	• Relative humidity • Wind speed • Solar radiation • Temperature of feed water, brine, ambient air • TDS of feed water and brine	• Water productivity	• ANN architecture: 9–20-1 • Hyper-parameter tuning method: Trial and error • Data split ratio: Train: 70%, validation:15%, and test: 15% • Different training methods were used namely LM, CGF, and RBP. • Results revealed that LM method had the best performance compared to other training methods.
[74]	2020	SS (single stage)	MLPANN	159	• Water temperature • Inner glass cover temperature	• Thermal conductivity • Partial vapor pressure • Volumetric expansivity • Specific heat • Latent heat of vaporization • Dynamic viscosity	• ANN architecture: 2–20-8 • Hyper-parameter tuning method: trial and error • Data split ratio: train: 70%, validation:15%, and test: 15% • Six different training methods including OSS, CGP, CGF, RBP, SCG, and LM were used for training the ANN model. • Results showed that the ANN model trained by the LM method had the best accuracy for the prediction of thermophysical properties of moist air in a SS.
[75]	2012	SS (single basin)	MLPANN	312, 453	• Insolation • Ambient temperature • Distillant volume • Wind speed • Wind direction • Daily average cloud cover	• Total daily distillate production	• ANN architecture: 6-20-1 • Hyper-parameter tuning method: trial and error • Data split ratio: SS A: train: 80%, validation: 5%, and test: 15%, SS B: train:80%, validation: 6%, and test: 14% • Two SS systems (A and B) were operated for a year and a half. • The minimum number of inputs for developing the ANN model was estimated. • It was concluded that the developed ANN model can effectively be used for performance prediction of other SS systems in different climate conditions, by using

(*continued on next page*)

Table 3 (*continued*)

Ref	Year	System type	Data-driven method	Dataset size	Inputs	Outputs	Main remark
							large experimental dataset for developing the ANN model.
[76]	2015	SS (single stage)	MLPANN	316	• Number of day (Julian day) • Relative humidity • Wind speed • Solar radiation • Ultra violet index • Feed, brine and ambient air temperature • TDS of feed and brine	• Water productivity • Operational recovery ratio • Thermal efficiency	• ANN architecture: 10-15-3 • Hyper-parameter tuning method: trial and error • Data split ratio: train: 70%, validation:10%, and test: 20% • The effect of each input parameter on the outputs was determined by the ANN model. • Temperature of the feed had the highest contribution for the prediction of water productivity and thermal efficiency of the SS. However, ultra violet index had the largest share in the prediction of operational recovery ratio.
[77]	2012	MD (VMD)	ANN	252	• Vacuum pressure • Feed inlet temperature • Feed salt concentration • Feed flow rate	• Permeate flux	• ANN architecture: 4-5-1 • Hyper parameter tuning method: GA • Data split ratio: train: 66%, validation: 17%, and test: 17%
[78]	2016	MD (VMD)	ANN	38	• Feed inlet temperature • Vacuum pressure • Feed flow rate • Feed salt concentration	• Permeate flux	• ANN architecture:4-3-1 • Hyper parameter tuning method: trial and Error • Data split ratio: train:70%, validation: 15%, and test: 15% • Parametric study using the developed ANN model showed that vacuum pressure and feed inlet temperature had the largest effect on the permeate flux, respectively.
[79]	2013	RO	SVR	3990	• Conductivity • Flow rate • Pressure	• Permeate flow rate • Permeate conductivity • Retentate flow rate • Retentate conductivity	• Data split ratio: train: 60%, and test: 40% • Steady state and transient models of a RO plant were constructed. • A time forecasting approach was proposed to show the temporal change in conductivity in transient operation. • It was concluded that the short-term performance forecasting models, could be used for process optimization, plant control algorithms, and fault tolerant control.
[80]	2021	SS integrated with thermoelectric modules	ANFIS-PSO, ANN-PSO	54	• Time • Fan power • Solar radiation • Ambient air, water, glass, and basin temperatures • Nanoparticle volume fraction	• Energy efficiency	• ANN architecture, ANFIS clusters: 8-3-1, 9 • Hyper-parameter tuning method: Trial and error • Data split ratio: train: 80% and test: 20% • Cu_2O nanoparticles were used in the SS basin. • PSO method enhanced the prediction performance significantly. • The ANFIS-PSO method had better performance compared to the ANN-PSO model.
[81]	2017	SS (single stage)	ANFIS	160	• Solar radiation • Relative humidity • TDS of feed • TDS of brine • Feed flow rate	• Water productivity	• Data split ratio: train: 70%, validation: 10%, and test: 20% • Sugeno-type fuzzy inference system was employed as the fuzzy interface system. • The grid partition method was applied for classification of the input data and creating the rules. • The Pi-shaped curve membership function outperformed the models with sigmoidal, triangular-shaped and trapezoidal-shaped MFs. • It was shown that solar radiation was the most influencing parameter on the SS productivity.
[38]	2016	RO	ANN	436	• Molecular weight • Compound hydrophobicity • Dipole moment • Molecular length • Molecular width • Salt rejection • Surface membrane charge • Membrane hydrophobicity • pH • Pressure • Temperature • Recovery	• Rejection rate	• The training dataset was re-sampled by a bootstrap method to form different training datasets. • Number of neurons in hidden layer were changed from three to 25. • Data split ratio: train: 80%, validation: 10%, and test: 10% • The BANN model outperformed the single neural network and BAMLR methods.

(*continued on next page*)

Table 3 (*continued*)

Ref	Year	System type	Data-driven method	Dataset size	Inputs	Outputs	Main remark
[82]	2018	RO	ANN, SVR, RF		• Feed temperature • Feed conductivity • Electrical power	• Pressure • Feed flow rate • Permeate flow rate • Permeate conductivity	• SVR and RF are significantly (5% significance level) better predictors of the plant's performances than ANN.
[83]	2020	SS (passive, active, and active SS integrated with a condenser)	ANN, ANN with HHO, SVR	72	• Solar irradiance • Ambient temperature • Time • Wind speed • Vapor velocity	• Water productivity	• ANN architecture: 5-5-15-1 • Hyper-parameter tuning method: Trial and error • Data split ratio: train: 70%, test: 30% • HHO-ANN showed the best accuracy compared to other models.
[39]	2013	Triple SS	ANN	46	• Time • Glass, plate and ambient air temperatures • Water temperature in the upper, middle and lower basins • Distillate volume • Solar intensity	Thermal efficiency	• ANN architecture: 9-10-1 • Hyper-parameter tuning method: Trial and error • Data split ratio: Train: 40%, validation:30%, and test: 30% • MLPANN showed the best predictive performance in comparison with NARX and ENN models.
[85]	2021	SS (stepped and conventional)	RNN (LSTM)	88	• Time	Hourly freshwater productivity	• Data split ratio: train: 72 datasets (9 days) and test: 16 datasets (2 days) • The freshwater production was used in a time series form to train the proposed model. • The accuracy of the proposed predictive model was compared with those obtained by conventional ARIMA and was evaluated using different statistical assessment measures. • The coefficient of determination of the predicted results has a high value of 0.99 and 0.97 for the stepped and conventional SS systems, respectively.
[86]	2020	RO	MLPANN-PSO, SVM, DT	150	• pH • Feed pressure • Temperature • Conductivity	Permeate TDS Permeate flow rate	• ANN architecture: 4-3-1 • The hybrid MLPANN-PSO model out-performed the SVM and DT (m5tree) models. • The hybrid model reached lower uncertainty for the simulated data.
[87]	2009	RO	ANN, SVR	10 min steps during 3 months	• Feed flow rate • Feed conductivity • Feed pressure • PH • Feed temperature • Permeate flow rate • Permeate conductivity • Permeate pressure	Permeate flux Salt passage	• Data split ratio: train: 40%, validation: 10%, and test: 50% • Various model architectures, memory time-intervals and forecasting times were used during the training process. • The concept of plant "short-term memory" time-interval was introduced to capture the time-variability of plant performance. • An actual state-of-the-plant model and two types of forecasting models (sequential forecasting and matching forecast) were studied using real-time RO plant performance data. • Results indicated good predictive accuracy for short-term memory time-intervals in the range of 8–24 h for permeate flux and salt passage for forecasting times up to 24 h.
[88]	2020	CDI	ANN, RF	600	• Physical structure related inputs (Specific surface area, pore volume, average pore size, channel pore volume) • Chemical structure related inputs (atomic content of nitrogen and oxygen) • Operational inputs (Applied voltage window, stream flow rate, NaCl salt concentration)	Electrosorption capacity of CDI	• ANN architecture: 9-10-1 • The contribution and relative importance of each feature were determined and validated.
[89]	2021	AD	ANFIS	15	• Cycle time • Switching time	• COP • SCP • SDWP	• Data split ratio: train: 66.66%, and test: 33.34% • The average RMSE value is decreased from 8.607 to 1.46 by using ANFIS instead of ANOVA.
[90]	2021	SS (double slope)		100	• Ambient air temperature	• Yield	

(continued on next page)

Table 3 (*continued*)

Ref	Year	System type	Data-driven method	Dataset size	Inputs	Outputs	Main remark
			RF, MLPANN, SVR, Linear SVR		• Wind speed • Solar radiation • Glass temperature • Vapor temperature • Basin water temperature		• Data split ratio: train: 70%, validation: 10%, and test: 20% • Hyper-parameter tuning method: Bayesian optimization algorithm • RF outperformed other models with the lowest absolute error percentage of 2.95%.

model had better performance compared to the empirical correlations, and thermodynamic models [66].

3.1.3. Comparison between different classical ML models

Choosing an appropriate ML model is highly important as there is no specific ML model that outperforms others in predicting the performance of desalination systems. Therefore, researchers have sought to compare the performance of different ML models developed by a similar dataset to achieve the best predictor. Khaouane et al. [38] reported that for a RO unit, the BANN model indicated better performance than the single neural network and bootstrap aggregated multiple linear regressions (BAMLR) methods. Also, it was shown that SVM and RF models were better predictors (5% significance level) of the RO plant's performance than neural networks [82]. However, for SS desalination systems, SVR models indicated weaker performance compared to the ANN Harris Hawks Optimizer (HHO) [83]. For MSF plants, it was reported that the RBFANN model performed better than the MLPANN model [66]. Similarly, RBFANN had a better forecasting performance compared to the ANN feedforward backpropagation model in evaluating the basin water temperature of SS systems [84]. Hamdan et al. [39] reported that the MLPANN had the best predictive performance for a SS system in comparison with NARX and ENN models. Moreover, Kandeal et al. [90] reported that RF outperformed the MLPANN and SVR methods in predicting the performance of double slope solar stills.

3.1.4. Use of DL models

Recently, LSTM, which is an RNN, was used in the DL field to predict the performance of stepped and conventional SS systems [85]. In this study, freshwater production was used in a time series form to train the proposed model. The accuracy of the proposed predictive model was compared with those obtained by conventional autoregressive integrated moving average (ARIMA) and was evaluated using different statistical assessment measures. It was shown that the predictive model for stepped-corrugated still has an R^2 value of 0.9752 and can be developed at a commercial scale to provide freshwater in remote areas.

These studies show that there is no single model that outperforms others under all conditions. This is due to the fact that the behavior of models is dependent on various factors from the hyper-parameters tuning and training methods to dataset size and split ratios, which are summarized below.

3.1.5. Training models and built-in functions

For ANNs, the training model and activation functions must be chosen appropriately. Aish et al. [65] reported that for a dataset obtained from a RO desalination unit, the MLPANN and RBFANN models have performed better when trained by the LM training method and backpropagation orthogonal least squares (OLS) algorithms, respectively. It was reported that the tangent hyperbolic and Gaussian radial basis activation functions in the hidden layer were led to the best performance in the MLPANN and RBFANN models. Also, different training methods were tested on performance prediction of SS processes and it was concluded that the LM method outperforms the conjugate gradient backpropagation with Fletcher Reeves restarts, and the RB training methods [73]. In another study on modeling SS process with ANNs, six different training methods of OSS, CGP, conjugate gradient Fletcher reeves update (CGF), RB, SCG, and LM were compared. Results indicated that training the ANN model with LM method led to the highest accuracy in predicting the thermophysical properties of moist air in a SS system [74]. For ANFIS model, the application of different membership functions (MF) was studied in [81]. It was reported that the Pi-shaped curve MF provides better and higher prediction accuracy than models with sigmoidal, triangular-shaped and trapezoidal-shaped MFs. In addition, the grid partition method was used for the classification of the input data and creating the rules.

3.1.6. Optimal training

Bahiraei et al. [67] used ICA and GA to train the MLPANN model in predicting the freshwater production of a SS system. It was shown that by using the GA and ICA algorithms, the root mean square error for test data decreased by 40.49% and 62.01%, respectively. In the continuation of the previous study [67], the ANFIS and ANN modeling of a SS desalination system fitted with thermoelectric modules was enhanced by particle swarm optimization (PSO) [80]. It was concluded that applying the PSO significantly enhances the energy efficiency prediction of the SS system. For water quality data obtained from three RO plants in Iran, it was shown that the hybrid MLP-PSO model outperformed the SVM and M5T models when predicting the permeate flowrate and total dissolved solids (TDS) [86].

3.1.7. Hyper-parameter tuning

Tuning the different hyper-parameters of the model is one of the important steps that affect the prediction performance. It can be seen from Table 3 that the majority of researchers used the trial and error approach for selecting the hyper-parameters, due to its simplicity and acceptable accuracy. The alternative method is applying optimization tools for the detection of the optimal hyper-parameters. Tavakolmoghadam and Safavi [77] used GA to optimize the ANN model parameters in predicting the performance of a VMD desalination system. The coefficients of the model, number of neurons and epochs were optimized by setting the population size of 80, crossover fraction of 0.9 and migration fraction of 0.1. It was observed that the network optimized by the GA, had the least errors (less than 1%) compared to the case with non-optimal parameters.

3.1.8. Dataset split ratio

It can be inferred from Table 3 that the majority of studies allocated 60–80% of the dataset to be used in training the models, while the remaining data is distributed between validation (0–33.3%) and test (5–40%) stages. This lies in the fact that without having an appropriate training dataset, the model will be faced with the underfitting problem. Therefore, a larger share of data is usually used to train the model. It is worth mentioning that further increase in the split ratio of the training stage has the risk of overfitting. On the other hand, it was reported that a RO unit [69] and a SS [39] trained with 33.3% and 40% of the dataset, also reached a determination coefficient of 0.97–0.99% and 90.36–99.87%, respectively. Libotean et al. [87] split the dataset obtained from a RO unit with a ratio of 40-10-50 percentages for train, validation and test stages, respectively. It was shown that the plant performance could be modeled with a reasonable level of accuracy, with a short-term memory interval of up to about 24 h.

3.1.9. Feature importance analysis (influential input and output parameters)

As different operational parameters affect the performance of desalination systems, selecting the most influential features as inputs and outputs are highly important. In modeling RO systems, parameters like temperature, pressure, conductivity, flow rate are the most common inputs, while some additional input parameters as recovery percentage [68], concentration [69], pH [65], membrane properties [38], and electrical power [82] were also considered. According to Table 3, the outputs in RO models have usually been selected among permeate flowrate, TDS and rejection rate. Kizhisser et al. [72] studied an RO plant from the economic viewpoint in which the parameters including the plant location, capacity, project financial type, and raw water salinity were considered as inputs to predict the capital cost of the plant. It was concluded that the proposed model provides a perspective to estimate the investment costs of the future RO plants. Saffarimiandoab et al. [88] studied a CDI desalination system by considering 9 operational and physical/chemical structure inputs and Electrosorption capacity of CDI as the single output. ANNs and RF models were examined and the contribution and relative importance of each feature was determined and validated. Regarding the SS systems, the inputs are mainly selected from parameters like solar radiation, wind speed, water depth, temperatures of water and glass, and ambient air. It was reported that solar radiation [81] and water temperature [76] had the highest contribution to the prediction of freshwater production. The minimum number of input parameters for developing the ANN model was estimated in [75] and it was concluded that the developed ANN model can effectively be used for performance prediction of other SS systems in different climate conditions with the aid of a large experimental dataset. Cao et al. [78] conducted a parametric study on a VMD desalination process by considering the vacuum pressure, feed inlet temperature, flow rate and salt concentration as inputs of the ANN model. Results revealed that the vacuum pressure and feed inlet temperature had the largest effect in predicting the permeate flux.

3.2. Performance prediction using design parameters

Unlike the studies in Table 3 that only considered operational

Table 4
Summary of studies on the performance prediction of desalination systems using design parameters.

Ref	Year	System type	Data-driven method	Dataset size	Inputs	Outputs	Main remarks
[91]	2015	RO	RBFANN	304	• Membrane properties (pore radius, friction constants between solute, solvent and membrane) • Model parameters (potential parameter, fractional pore area, average pore length) • Operational parameters (average longitude concentration of solute in membrane, pressure, and temperature)	• Separation factor • Pure solvent flux • Total flux	• ANN architecture: 9-20-1 • Hyper parameter tuning method: Trial and error • Data split ratio: train: 80%, and test: 20% • RBFANN outperformed the previous mathematical and mechanism base models.
[92]	2019	HDH (solar seawater greenhouse)	ANN	66	• Width, length, the height of the front evaporator • Roof transparency	• Desalinated water production rate	• ANN architecture: 4-9-1 • Hyper parameter tuning method: Trial and error • Data split: train: 70%, validation: 15%, and test: 5% • Different algorithms such as the conjugate gradient algorithm, the gradient descent algorithm, the BFGS algorithm, Bayesian, and the LM algorithm were used to train the ANN model. • The best training algorithm was the LM algorithm.
[40]	2020	HDH (seawater greenhouse system)	MLPANN	30	• Width, length, the height of the front evaporator • Roof transparency	• Power consumption • Water productivity	• Data split: train: 70% and test: 30% • The performance of the RVFL network, which is a MLPANN, integrated with artificial ecosystem-based optimization (AEO) algorithm was compared with that of the conventional RVFL model. • RVFL-AEO showed a better performance compared with RVFL, indicating the role of AEO in obtaining the optimal RVFL parameters that enhances the accuracy of the model.
[93]	2018	HDH (seawater greenhouse system)	SVR	66	• Greenhouse width and length • First evaporator height • Roof transparency	• Water production • Energy consumption	• Data split: train: 70% and test: 30% • The effect of each input parameter on water production and energy consumption was studied using the developed model.
[94]	2020	MD (VMD)	ANN	36	• Feed inlet temperature • Feed flow rate • Membrane length	• Permeate flux • Specific heat energy consumption	• ANN architecture: 3-7-1 • Hyper-parameter tuning: Trial and error • Data split ratio: train:70%, validation: 10%, and test: 20% • As feed inlet temperature and feed flow rate increased, the permeate flux increased. Further, with an increase in membrane length, the permeate flux decreased. • Specific heat energy consumption increased for longer membranes and declined with and an increase in temperature and mass flow rate of feed flow.

parameters, Table 4 shows the studies that have also included design parameters in their model inputs when predicting the performance of desalination systems. It can be seen that only a limited number of investigations have used the design parameters to predict the performance of desalination systems. Iranmanesh et al. [91] compared the performance of the RBFANN method with the mathematical surface force pore flow model to predict the performance of the RO system. By using different membrane properties, model parameters, and operational parameters, their results showed that the RBFANN method had better accuracy than the mathematical approach. In the case of HDH systems, three studies can be found in the literature that aimed to employ the ANN and SVR methods to anticipate the performance of the seawater greenhouse systems by considering geometrical parameters as model inputs [40,92,93]. Zarei and Behyad [92] studied the accuracy of different training algorithms for the ANN model. It was concluded that the Levenberg-Marquardt training algorithm had superiority over the other training methods. The results reported by Essa et al. [40] highlighted the important role of accurate hyper-parameter tuning methods in ML methods for performance analysis of HDH systems. The results showed that coupling the RVFL model with the artificial ecosystem-based optimization algorithm enhanced the accuracy of the model. In another study [93], the application of the SVR model for performance analysis of a seawater greenhouse system was analyzed and results showed the great capability of the developed model to predict the freshwater production rate as well as energy consumption. In the case of MD systems, the membrane length of VMD configuration along with operational parameters of feed flow (mass flow rate and temperature) were taken into account as the inputs for developing the ANN model [94]. This study revealed that the membrane length had a significant effect on both permeate flux and energy consumption, thus the vital importance of considering the membrane length as an input for developing the data-driven methods.

3.3. Optimization and correlation development

Table 5 indicates the studies that employed data-driven methods for optimization and correlation generation in desalination systems. In these studies, either operational/design or both of these parameter types were considered as inputs. Compared to Sections 3.1 and 3.2, the optimization and correlation development is also taken into account in this section. The main remarks of Table 5 can be summarized as follows:

- Among different desalination systems, data-driven methods have been mostly used to optimize and generate correlations in SS and MD desalination methods.
- Water productivity was mainly considered as the output target for optimization and correlation generation in desalination systems.
- To optimize the performance of various desalination systems using data-driven methods, design parameters as the inputs have been received less attention compared to the operational parameters. Limited studies confirmed that the interaction of operational and design parameters has a significant effect on the performance of desalination systems [59,95–99].
- The RSM method has been broadly employed for the optimization of desalination systems compared to ML models. The main reason is that the RSM method mainly requires a lower number of data than ML methods to optimize the performance of the system. However, it can be seen in a few comparative studies that ML models mainly enjoyed better performance prediction than the RSM method [14,100]. This shows that coupling the ML models with optimization methods such as GA, PSO, and Monte Carlo can lead to enhanced optimization results.
- Minitab, Design expert and Statistica software have been used for developing the RSM method whereas MATLAB was the most commonly used software to optimize the desalination systems using ML methods.
- Correlations have been mostly generated using the quadratic polynomial model obtained by RSM and linear regression models such as stepwise and multiple linear regression methods. However, it can be inferred from Table 5 that ML models outperformed these correlations for performance prediction of desalination systems [101–106].
- Limited studies have been conducted on the application of data-driven methods for optimization and correlation development of solar-driven HDH and MD systems. In the case of HDH desalination systems, RSM method was employed to optimize the freshwater generation of vacuum humidification dehumidification (VHD) systems [107,108]. Moreover, design parameters only were considered in limited studies for optimization of HDH systems [109,110].
- The accuracy of the developed correlations for SS systems was compared with the estimated values by the computational fluid dynamics (CFD) method. The results showed a close agreement between the obtained values and confirmed the robustness of the developed correlations [111,112].

3.4. Maintenance

Table 6 shows a summary of studies that have applied data-driven methods to analyze the fouling and wetting phenomena in membrane-based desalination systems. Fouling is a serious issue in all membrane desalination technologies and its accurate prediction plays a vital role in performance improvement, cost reduction, and sustainability of these systems. Fouling mechanism is generally defined as the deposition of undesired materials (solid particles in the feed stream, ions, and biological materials) on the membrane surface and inside the pores, resulting in lowering the permeate flux over time [143] which increases the cost of produced water [144]. The conventional mechanistic modeling methods have failed to accurately predict the fouling mechanism in different membrane-based desalination technologies mainly due to the dynamic nature of the fouling phenomenon, the complexity involved in the mathematical approach, and developing the models based on several simplified assumptions [6,145,146]. As a result, data-driven methods have gained more attention and researchers have sought to employ these methods for precise prediction of the fouling mechanism. Liu and Kim [147] compared the performance of ANN and mathematical models (blocking laws) to foresee the transmembrane pressure drop in the MD system due to the fouling effect. The results showed a great superiority of the ANN model over the blocking laws approach. Recently, Mittal et al. [6] showed the viability of the ANN model to analyze the effects of operational parameters of the VMD module on the permeate flux decline as a result of membrane fouling. The robustness of the ANN model for membrane fouling analysis has also been supported for RO [148] and electrodialysis [149] desalination systems.

The possibility of employing the CNN model for studying the fouling mechanism in desalination systems has also been investigated in several studies. The performance of the CNN model for studying the fouling effect in a RO desalination system was compared with that of the mathematical model by Park et al. [145]. They used 4000 images for testing the performance of the developed CNN model and the results showed that the CNN model had better performance than the mathematical model. In another study, fouling characteristics of a membrane used for the FO desalination method was comprehensively analyzed by the CNN model and results showed great performance of CNN model for the prediction of thickness, porosity, roughness, and density of the fouling layer.

Membrane wetting is another serious issue with the MD desalination technology and this mainly stems from membrane fouling and high liquid entry pressures [150]. Due to the interaction effects of operational parameters and membrane characteristics on the wetting problem, accurate prediction of membrane wetting using mathematical models is complex and tedious. Recently, Kim et al. [151] examined the predictive performance of RSM and ANN models to investigate the wetting issue of

Table 5
Summary of studies on the application of data-driven methods for optimization and correlation development.

Ref	Year	Optimization	Correlation	System type	Data-driven method	Dataset size	Inputs	Outputs	Main remark
[95]	2020	✓	✓	SS (different configurations of active SS)	FD	Not mentioned (n.m.)	• Basin area • Depth of saline water • External power • Air blowing system • Condenser material • Condenser thickness • Condenser area • Insulation thickness • Insulation material • Ambient air temperature • Make-up water system	• Distilled water • Saline water temperature • Condenser cover temperature	• Design method: factorial • The most influencing input parameters on the distilled water were the external power, the depth of the saline water, and the basin area of the active still, respectively.
[96]	2021	✓	✓	SS (Single stage)	RSM	30	• Solar radiation • Ambient temperature • Water depth • Thickness of insulation	• Daily freshwater productivity	• Design method: CCD • Water depth, solar radiation, ambient temperature, and thickness of insulation had the largest effect on the daily freshwater productivity, respectively.
[97]	2016	✓	✓	MD (DCMD)	RSM	36	• Inlet temperatures of feed and permeate • Flow velocity of feed • Module packing density • Length-diameter ratio of module	• Permeate flux • Water productivity per unit volume of module • water production per unit energy consumption • Comprehensive index to find out a balance among high water flux, high production, and low energy consumption	• Design method: QRCD • Multi-objective optimization was also performed to maximize the permeate flux and minimize energy consumption. • The permeate flux was mainly affected by feed inlet temperature and its interactions with length-diameter ratio of module.
[98]	2020	✓	✓	MD (DCMD)	RSM	36	• Inlet temperatures of feed and permeate • Flow velocity of feed solution • Module packing density • Length-diameter ratio of module	• Feed/permeate side heat transfer coefficients • Temperature polarization coefficient • Permeate flux • Water productivity per module volume • Thermal efficiency	• Design method: QRCD • Multi-objective optimization was also made using the RSM method. • Theoretical heat and mass transfer models were coupled with the RSM technique to determine the complex interaction effects of inputs on the outputs. • Higher feed temperatures, shorter membranes, and higher feed velocities led to a significant increase in the heat transfer coefficients, thereby enhancement of permeate flux and thermal efficiency.
[99]	2018	✓	✓	MD (VMD)	RSM	36	• Temperature • Velocity • Concentration of feed flow	• Water permeate flux • Water productivity per	• Feed inlet temperature and its interaction had a significant effect on

(continued on next page)

Table 5 (*continued*)

Ref	Year	Optimization	Correlation	System type	Data-driven method	Dataset size	Inputs	Outputs	Main remark
							• Membrane packing density • Length–diameter ratio of module	unit volume of module • GOR • Comprehensive index	VMD module performance. • As module packing density increases, water productivity per unit of the module rises, but GOR remained relatively unchanged. • The increase in packing density led to a decrease in water permeate flux, whereas resulted in an increase in water productivity per unit of the module, which is a more important index for practical applications.
[59]	2016	✓	✓	MD (AGMD)	RSM and TM	27	• Feed flow rate • Feed temperature • Coolant temperature • Coolant flow rate • Air gap width	• Permeate flux	• Design method: FCCD • Optimization was also performed using RSM and Taguchi techniques. • Air gap width and temperature of feed flow had significant effect on the permeate flux of AGMD system. • Compared to other input variables, coolant flow rate had insignificant effect on the permeate flux. • Both RSM and Taguchi techniques provided an accurate prediction of permeate flux. However, RSM outperformed the Taguchi method and was recommended as a better tool for performance prediction and optimization of the AGMD system.
[14]	2010	✓	✓	RO	MLPANN & RSM	26	• Sodium chloride concentration in feed solution • Feed temperature • Feed flow rate • Operating hydrostatic pressure	• RO performance index (=salt rejection factor times the permeate flux)	• ANN architecture: 4-5-3-1 • Data split ratio: train: 66%, validation: 17%, and test: 17% • Two empirical polynomial RSM models valid for different ranges of feed salt concentrations were performed (in MATLAB). However, the developed ANN model was valid over the whole range of feed salt concentration.

(*continued on next page*)

Table 5 (*continued*)

Ref	Year	Optimization	Correlation	System type	Data-driven method	Dataset size	Inputs	Outputs	Main remark
									• ANN has the ability to overcome the limitation of the quadratic polynomial model obtained by RSM. • Analysis of variance (ANOVA) has been used to test the significance of response surface polynomials and ANN model. • The optimum operating conditions were found by Monte Carlo simulations.
[100]	2018	✓	✓	Permeate gap membrane distillation (PGMD)	RSM & ANN	RSM: 26 ANN: 88	• Condenser inlet temperature • Evaporator inlet temperature • Feed flow rate • Feed water salt concentration	• Permeate flux • Specific Thermal Energy Consumption	• ANN architecture: 4–7–2-2 • Hyper-parameter tuning method: Trial and error • Data split ratio: train: 75%, validation: 20%, and test 5% • Design method: FCCD • Multi-objective optimization was made using non-dominated sorting genetic algorithm (NSGA-II). • The ANN model outperformed RSM for performance prediction of the PGMD module. • Developing the ANN model required more experimental data compared to the RSM.
[101]	2017	✘	✓	SS (single stage)	ANN & RM	160	• Ambient temperature • Relative humidity • Wind speed • Solar radiation • Feed flow rate • Temperature of feed water • Total dissolved solids in feed water	• Water productivity	• ANN architecture: 7-8-1 • Hyper-parameter tuning method: Trial and error • Data split ratio: train: 70%, validation:10%, and test: 20% • Compared with the stepwise regression model, the ANN model showed a greater performance for the prediction of water productivity.
[102]	2019	✘	✓	SS (single stage)	ANN, ANFIS, and RM	160	• Relative humidity • Solar radiation • Feed flow rate • Total dissolved solids of feed and brine	• Water productivity	• ANN architecture: 5-10-1 • Hyper-parameter tuning method: Trial and error • Data split ratio: train: 70%, validation:10%, and test: 20% • Results showed that ANN, ANFIS, and multiple regression models could accurately predict

(continued on next page)

Table 5 (*continued*)

Ref	Year	Optimization	Correlation	System type	Data-driven method	Dataset size	Inputs	Outputs	Main remark
									the water productivity, but the ANN model outperformed the other models.
[103]	2016	✘	✓	SS (single stage)	ANN and RM	160	• Julian day • Ambient air temperature • Relative humidity • Wind speed • Solar radiation • Temperature of feed water • Temperature of brine water • Total dissolved solids (TDS) of feed water • Total dissolved solids (TDS) of brine water	• Thermal efficiency	• ANN architecture: 9-12-1 • Hyper-parameter tuning method: Trial and error • Data split ratio: train: 70%, validation:10%, and test: 20% • The ANN model showed a better predictive performance compared to multi-variate regression and stepwise regres-sion models.
[104]	2021	✘	✓	Tubular SS	ANN, RF, RM	16 days	• Solar radiation intensity • Wind speed • Temperatures of basin plate, salt water, cover, and ambient air	• Hourly freshwater Production	• ANN architecture: 6-56-202-681-1 • Hyper-parameter tuning method: Bayesian optimization algorithm • Data split ratio: train: 80% and test: 20% • A comparison was made among ANN, RF, and traditional multilinear regression models. • Application of Bayesian optimization algorithm for hyper-parameter tuning process enhanced the performance of the ANN model by 35%. • RF model was less sensitive to hyper-parameter tuning compared to the ANN model. • Feature importance analysis revealed that saltwater temperature, basin temperature, and solar radiation were the most influencing parameters, respectively. • The RF model was recommended as the ML model for performance prediction of tubular SS mainly due to its high accuracy and robustness.
[105]	2017	✘	✓	SS (single stage)	ANN & RM	56	• Ambient air temperature • Relative humidity • Wind speed • Solar radiation • Flow rate • Temperature	• Instantaneous thermal efficiency	• ANN architecture: 7-6-1 • Hyper-parameter tuning method: Trial and error • Data split ratio: train: 70%,

(continued on next page)

Table 5 (*continued*)

Ref	Year	Optimization	Correlation	System type	Data-driven method	Dataset size	Inputs	Outputs	Main remark
							• Total dissolved solids of feed water		validation:10%, and test: 20% • Agricultural drainage water as a non-conventional source of water was used as the feed water into the SS system. • Results showed that the ANN model had a better performance than multiple linear regression for the prediction of thermal efficiency.
[106]	2018	✘	✓	MD (PGMD)	ANN & RM	Electric test: 372 Solar test: 11272 Both: 11644	• Temperatures at the condenser and evaporator inlets • Feed seawater flow	• Permeate flux	• ANN architecture: 3-10-1 • Hyper –parameter tuning method: Trial and Error • Data split ratio: train: 90%, validation: 5%, and test: 5% • Three datasets for training the ANN were considered: 1. electrical test, 2. Solar test. 3. Both electrical and solar tests • ANN outperformed linear regression.
[107]	2018	✓	✘	HDH (solar VHD)	RSM	15	• Humidifier pressure • Inlet water temperature • Ratio of water to air mass flow rates	• Desalinated water production rate	• To increase the water productivity, the pressure of the humidifier was lower than atmospheric pressure using a vacuum pump. • Optimum values of inputs were determined by the RSM analysis
[108]	2021	✓	✘	HDH (three stage VHD)	RSM	20	• Air temperature • Water to air mass flow rate • Humidifiers pressure	• Desalinated water production rate	• Design method: FCCD • Optimum values of inputs were achieved by the RSM analysis. • The freshwater productivity of a three-stage vacuum HDH was compared with a single-stage vacuum HDH sys-tem. Three-stage system had higher productivity and lower energy consumption.
[109]	2011	✓	✓	HDH (C/OAOW-AWH)	FD	2 k = 6 = 64 And 3 k = 6 = 729	• Inlet water temperature • Inlet air temperature • Input heat flux • $A_{cond}U_{cond}$ • Water mass flow rate • Air mass flow rate	• Freshwater production	• Design method: factorial • Thermodynamic model was used and DOE analysis was performed for sensitivity analysis and optimization purposes. • A correlation was developed for the

(*continued on next page*)

Table 5 (*continued*)

Ref	Year	Optimization	Correlation	System type	Data-driven method	Dataset size	Inputs	Outputs	Main remark
									prediction of freshwater productivity based on the input variables.
[110]	2016	✓	✓	HDH (solar humidifier and a subsurface condensation mechanism)	RSM	282	• Inflowing air temperature • Length of condenser tube • Relative humidity of inflowing air • Inflowing air velocity • Cross-section of inflowing air • Height of water in evaporation still • Solar radiation • Temperature of water in evaporation still	• Freshwater productivity	• Design method: CCD • Solar energy was the main heat source and a set of tubes buried in the soil acted as condensers • Water temperature variation of solar humidifier had the most contribution to freshwater productivity. • Correlation was developed for forecasting freshwater productivity.
[111]	2016	✓	✓	SS (single stage)	RSM	13	• Position and size of the partition	• Nusselt number	• Design method: CCD • Both CFD and RSM methods were employed. • The partition was placed at the bottom surface and glass cover of the still for performance improvement of the SS. • The RSM provided great predictive performance as compared to the CFD model. The maximum error for the prediction of bottom and top normalized Nusselt numbers were 1.3%.
[112]	2018	✓	✓	Stepped SS with nanofluids in basin	RSM	13	• Height and length of the steps inside the cascade SS	• Hourly productivity	• Design method: CCD • Both RSM and CFD analyses were used to predict the hourly productivity of the SS system. • The RSM showed a great predictive performance, only a 2.1% difference was reported between the estimated values by RSM and CFD methods.
[113]	2009	✓	✘	MSF-RO	ANN	200	• Feed temperature • Feed total dissolved solids • *Trans*-membrane pressure • Feed flow rate • Time	• Permeate TDS • Permeate flow rate	• ANN architecture: 5–15–1 • Data split ratio: train: 60%, validation: 20%, and test: 20% • A framework for developing an ANN model was proposed to predict the performance and optimizing the operation of SWRO desalination plants. • It was concluded that ANNs could be combined with deterministic

(*continued on next page*)

Table 5 (*continued*)

Ref	Year	Optimization	Correlation	System type	Data-driven method	Dataset size	Inputs	Outputs	Main remark
									models that include physical laws as a hybrid model for studying fouling/ scaling and process optimization in RO systems.
[114]	2019	✓	✘	RO	RNN	Historical data from 2015 to 2017	• Ambient temperature • Solar radiation • Wind speed • Water demand	• Freshwater production	• RNN was used to predict the future energy supply from renewable sources, and water demand • Multi-criteria optimization was done using extended mathematical programming to minimize the total annual costs and greenhouse gas emission. • The potential loss of power supply probability was introduced as a tool to illustrate the sustainability of the proposed scenarios. • It was concluded that the advanced forecasting algorithms could address future uncertainties in the energy supply chain.
[15]	2016	✓	✘	FO	Taguchi–neural	16	• Feed solution velocity • Draw solution • Velocity • Feed solution temperature • Draw solution temperature	• Maximum reverse solute flux selectivity	• ANOVA was used to detect the main parameters that could affect FO quality characteristics. • MINITAB software version 16 was used to solve Taguchi and ANOVA methods and the STATISTICA 12 software was used to carry out training, validation, and testing of the neural network.
[115]	2014	✘	✓	RO	ANN	370	• Time • Concentration • Operating pressure • Membrane type	• Water permeability constant	• ANN architecture: 4-4-1 • Data split ratio: train: 50%, validation: 25%, and test: 25% • The proposed time dependent neural network based correlation can predict the water permeability constant. • For the first time, the effect of feed salinity on water permeability constant values at low-pressure operation is reported.
[116]	2021	✓	✓	RO	RSM & ANN	30	• Feed concentration • Temperature • pH • Pressure	• Permeate flux • Water recovery • Salt rejection	• RSM and ANN models were statistically studied using ANOVA.

(*continued on next page*)

Table 5 (*continued*)

Ref	Year	Optimization	Correlation	System type	Data-driven method	Dataset size	Inputs	Outputs	Main remark
								• Specific energy consumption	• Numerical optimization of NF and RO pilot plant was done to attain the optimum conditions. • By using the optimum conditions, three hybrid configurations of NF and RO were analyzed to determine the best mode for the treatment of brackish groundwater.
[117]	2021	✓	✓	FO	ANFIS, ANN, RSM	50	• Draw concentration • Feed concentration • Time • Feed pH • Feed temperature	• Water flux • Reverse salt flux	• Data split ratio: train: 70%, validation: 15%, and test: 15% • ANN and RSM models were considerably better than ANFIS.
[16]	2021	✓	✓	FO	ANN & RSM	76	• Osmotic pressure difference • Feed solution velocity • Draw solution velocity • Feed solution temperature • Draw solution temperature	• Membrane flux	• A BBD is used to develop a response surface design where the ANN model evaluates the responses. • The weights of the ANN model and the response surface plots were used to optimize and study the influence of the operating conditions on the membrane flux.
[118]	2016	✓	✓	FO	RSM	16	• Feed flow rate • Permeate flow rate • Permeate temperature	• Permeate flux • FO specific performance index	• A Monte Carlo Simulation method has been conducted to determine the optimum operating conditions of the FO pilot plant.
[119]	2020	✘	✓	FO	ANN and RM	709	• Membrane type • Orientation of membrane • Molarity of feed solution • Molarity of draw solution • Type of feed solution • Type of draw solution • Crossflow velocity of the feed solution • Draw solution • Temperature of the feed solution • Temperature of the draw solution	• Permeate flux	• ANN architecture: 9-25-25-40-1 • Data split ratio: train: 70%, validation: 15%, and test: 15% • ANN formed a better relationship between inputs and output than multiple-linear regression model. • The performance of the ANN model is compared with a transport-based model in the literature.
[120]	2020	✓	✘	SS (single and stepped basin type)	TM	9	• Basin liner design • Heat storage material • Wick material • Basin water depth	• Water production	• Design method: L9 orthogonal array • Optimum values of inputs were determined using the Taguchi method. • Compared to the conventional single and stepped basin SS

(continued on next page)

Table 5 (*continued*)

Ref	Year	Optimization	Correlation	System type	Data-driven method	Dataset size	Inputs	Outputs	Main remark
									systems, water productivity increased by 175.2% and 132.2% for the single basin and stepped basin SS when the TM was employed.
[121]	2016	✓	✘	SS (single stage active type)	RSM	29	• Latent heat materials • Different sensible materials • Evaporation surfaces • Different types of heat transfer in the still	• Freshwater productivity • Efficiency	• Design method: BBD • Biomass heat source was used as the main heat source.
[122]	2020	✘	✓	SS (single stage)	MLPANN	48	• Time • Solar radiation • Ambient air, glass, basin and water temperatures	• Energy efficiency • Exergy efficiency • Water productivity	• ANN architecture: 6-5-3 • Hyper-parameter tuning method: Trial and error • Data split ratio: train:80% and test:20% • ICA as an optimization algorithm was employed for minimization of cost function of ANN model. • Applying the ICA optimization for ANN model enhanced the predictive performance of ANN model significantly.
[123]	2019	✘	✓	SS (double slope single basin in active and passive mode)	FD	24	• Glass temperature • Bottom temperature	• Water temperature	• Bottom temperature had the largest contribution to increasing the water temperature in the basin. • The interaction of inputs had an insignificant effect on the water temperature.
[124]	2018	✘	✓	Stepped SS	ANN & RM	n.m.	• Solar radiation • Ambient temperature • Month number • Day number • Number of hours per day • Wind speed • Humidity • Cloud cover • Vapor temperature • Water and basin temperatures • Difference between the inner and outer surface of glass temperature	• Water productivity	• ANN architecture: 12-27-1 • Hyper-parameter tuning method: Iterative optimization • Data split ratio: train: 70% and test: 30% • Hourly experimental data for three months was collected. • Results showed that cascaded forward neural network model had superiority over the linear regression and multiple-linear regression models.
[125]	2020	✓	✓	SS (conventional type integrated with a parabolic	RSM	n.m.	• Saline water and glass cover temperatures	• Water productivity	• Design method: BBD • Principal component analysis was initially

(*continued on next page*)

Table 5 (*continued*)

Ref	Year	Optimization	Correlation	System type	Data-driven method	Dataset size	Inputs	Outputs	Main remark
				trough collector)			• Dry bulb temperature • Wet bulb temperature inside the conventional SS • Ambient air temperature • Oil inlet temperature • Solar intensity		performed to decrease the number of inputs for conducting the RSM analysis. • Principal component analysis showed that three groups of inputs had the largest effect on water productivity: 1: (saline water temperature, wet bulb temperature, and dry bulb temperature), 2: (solar intensity, ambient air temperature, and glass cover temperature), 3: (ambient air temperature, oil inlet temperature, and solar intensity). • These three categories of inputs were then used for the RSM analysis. • Results showed that solar intensity, ambient air temperature, and glass cover temperature had a significant effect on water productivity.
[126]	2020	✘	✓	Concave type Stepped SS	RM	n.m.	• Solar radiation • Basin, glass, water, and ambient air temperature and	• Hourly water production	• Locally available material such as bricks, sand, and concrete pieces were used in SS to extend the time of water productivity and therefore increasing water productivity. • Linear regression model was used.
[127]	2014	✓	✓	MD (AGMD)	RSM	20	• Cold & hot feed inlet temperature • Feed-in flow rate	• Permeate flux • GOR	• Design method: CCD • Optimal operating parameters were determined by NSGA-II. • Results showed that hot feed inlet temperature had the largest positive effect on both permeate flux and GOR.
[128]	2020	✓	✓	MD (AGMD)	RSM and TM	16	• Feed temperature • Feed flow rate • Salinity	• Permeate flux • Energy consumption	• Lower feed temperatures and higher feed flow rates resulted in higher permeate flux with a lower energy cost.
[129]	2007	✓	✓	MD (DCMD)	RSM	16	• Stirring rate • Feed temperature • NaCl concentration in the feed solution	• Permeate flux	• Design method: CCD • Canonical analysis was used for optimization purposes. • A gradient method was employed to find the response

(continued on next page)

Table 5 (*continued*)

Ref	Year	Optimization	Correlation	System type	Data-driven method	Dataset size	Inputs	Outputs	Main remark
									surface within the domain of experimentation.
[130]	2018	✓	✓	MD (AGMD)	RSM	16	• Evaporator inlet temperature • Condenser inlet temperature • Feed flow rate	• Permeate flux • Specific thermal energy consumption • GOR	• Design method: FCCD • Multi-objective optimization was performed. • Two modules with different areas were used: 7.2 m^2 and 24 m^2 • In the case of the longer module, there was an optimum condition that led to highest productivity and the highest thermal efficiency. However, for the shorter module, there was a trade-off between reaching the highest productivity and the highest thermal efficiency.
[131]	2017	✓	✓	MD (PGMD)	RSM	16	• Evaporator and condenser inlet temperatures • Feed flow rate	• Permeate flux • Specific thermal energy consumption	• Design method: FCCD • Multi-objective optimization was performed. • Evaporator inlet temperature had the largest effect on permeate flux and specific thermal energy consumption. However, condenser inlet temperature had insignificant effects on both permeate flux and specific thermal energy consumption.
[132]	2012	✓	✓	MD (SGMD)	RSM	26	• Liquid and gas temperatures • Liquid and gas flow rates	• Permeate flux	• Design method: CCD • Monte Carlo method was used for the optimization purpose. • The interaction effect of the air circulating velocity and the air inlet temperature was highlighted. • A higher permeate flux was obtained by lower air inlet temperatures and higher air flow rates.
[133]	2012	✓	✓	MD (AGMD)	RSM	16	• Feed inlet temperature • Cooling inlet temperature • Feed flow rate	• Permeate flux • Salt rejection factor • Energy consumption	• Design method: CCD • The Monte Carlo technique was used for optimization. • Feed inlet temperature had the largest effect on performance of AGMD system.
[134]	2014	✓	✓	MD (DCMD)	RSM	28	• Vapor pressure difference • Feed flow rate	• Permeate flux	• Design method: CCD • For the optimum working condition,

(*continued on next page*)

Table 5 (*continued*)

Ref	Year	Optimization	Correlation	System type	Data-driven method	Dataset size	Inputs	Outputs	Main remark
							• Permeate flow rate • Feed ionic strength		there was a 3.9% deviation between the prediction and the actual experimental value, which showed the validity of the developed model.
[135]	2017	✓	✓	MD (AGMD)	RSM	25	• Hot and cold feed inlet temperatures • Feed flow rate • Feed conductivity	• Permeate flux • Specific performance ratio	• Design method: CCD • Hot feed inlet temperature had the largest positive effect on the permeate flux of the AGMD module followed by the feed flow rate.
[58]	2016	✓	✓	MD (DCMD)	RSM	28	• Feed temperature • Cold flow temperature • Feed flow rate • Cold flow rate	• Permeate flux	• Design method: CCD • Feed temperature, feed flow rate, and cold flow rate had a positive effect on permeate flux. However, increasing the cold flow temperature resulted in a decrease in permeate flux.
[136]	2015	✓	✓	MD (VMD)	RSM	27	• Feed temperature • Vacuum pressure • Feed flow rate • Feed concentration	• Permeate flux	• Design method: Box–Behnken • Vacuum pressure has the largest effect on the permeate flux followed by feed temperature and feed concentration. • Feed flow rate had relatively no effect on the permeate flux.
[137]	2017	✓	✓	MD (AGMD & water gap membrane distillation)	Genetic programming & ANN	154	• Feed temperature • Feed concentration • Feed flow rate • Coolant flow rate	• Permeate flux	• Data split ratio: train: 75% and test: 25% • Feed temperature was the most influencing parameter on the permeate flux. • Generic programing had a better predictive performance than ANN according to the coefficient of the determination index.
[138]	2020	✓	✓	MD (VMD)	RSM	20	• Feed inlet temperature • Feed flow rate • Vacuum pressure	• Permeate flux • Energy consumption	• Design method: CCD • Solar thermal-photovoltaic VMD system was studied.
[139]	2009	✓	✓	MD (DCMD & AGMD)	RSM	DCMD:25 AGMD:9	DCMD: • Hot fluid flowrate • Hot fluid temperature • Cold fluid flowrate • Membrane thickness AGMD: • Hot fluid flowrate • Hot fluid temperature	• The rate of water produced per unit hot liquid feed rate • Auxiliary heat input	• Design method: CCD • Optimization was performed using Aspen Plus software and RSM technique.
[140]	2012	✓	✘		ANN	72	• Air gap thickness	• Distillate flux	

(continued on next page)

Table 5 (*continued*)

Ref	Year	Optimization	Correlation	System type	Data-driven method	Dataset size	Inputs	Outputs	Main remark
				MD (AGMD)			• Condensation temperature • Feed inlet temperature • Feed flow rate of salt aqueous solutions	• Salt rejection factor	• ANN architecture: 4-10-1 • Hyper-parameter tuning: Trial and Error • Data split ratio: train:75%, validation: 16%, and test: 9% • Monte Carlo simulation was employed for optimization. Feed inlet temperature had the largest effect on the AGMD module performance.
[141]	2013	✓	✘	MD (SGMD)	ANN	53	• Feed inlet temperature • Feed flow rate • Air flow rate	• Distillate flux • Salt rejection factor	• ANN architecture: 3–9-1 • Hyper-parameter tuning: trial and error • Data split: train: 80%, validation: 10%, and test:10% • Monte Carlo simulation was employed for optimization. • Parametric study using the ANN model showed that the inlet feed temperature and sweeping air flow were the most influencing parameters. However, the liquid flow rate had insignificant effect on the SGMD performance.
[142]	2021	✓	✘	CDI	ANN & RF	2364	• Operational features (electrolyte NaCl concentration, electrolyte flow rate, applied voltage window) • Electrode features (Electrode specific surface area, micropore volume, channel pore volume)	• Desalination capacity • Speed • Time	• Data split: train: 90%, and test:10% • Activation function: rectified linear unit • A 10-fold grid-search cross-validation was performed for every model to optimize the network structure and hyper-parameters with respect to the models' accuracy in terms of an objective function. • The number of decision trees and their maximum depth were optimized by 10-fold grid-search cross-validation. • Every instance of the features was analyzed using latest model interpretation techniques (the SHapley Additive exPlanations, the

(continued on next page)

Table 5 (*continued*)

Ref	Year	Optimization	Correlation	System type	Data-driven method	Dataset size	Inputs	Outputs	Main remark
									Individual Conditional Expectation, the Partial Dependence Plots, and the Mean Decrease Impurity) to determine the time variation of features contribution.

the DCMD system and the findings showed that both models can be effectively applied for analysis of the wetting phenomenon in the DCMD configuration.

3.5. Control

Table 7 summarizes the studies on the application of data-driven methods for controlling the performance of various desalination systems. It can be seen that the ANN model as a great performance predictive modeling tool of non-linear systems, has received researchers' attention for controlling purposes. Moreover, the obtained results reported in [34] showed that the LSTM deep learning model can be effectively applied for the dynamic control of RO desalination systems. As can be seen from Table 7, despite the intermittent nature of wind and solar energies, insufficient investigations have been conducted on the application of data-driven controlling methods for performance improvement and cost reduction of renewable-based desalination systems. Cabrera et al. [152] showed the excellent capability of the ANN model in controlling the variable operation of a standalone wind-driven RO desalination plant. In another study [153], applying the reinforcement learning model led to a 14% cost decline in a renewable-based RO desalination technology. Similarly, Gandhi et al. [154] reported that the sequential extreme learning method can be successfully applied for performance improvement and cost reduction of the SS desalination system. With adapting control of feed mass flow rate using the ANN model, Porrazzo et al. [155] enhanced the daily freshwater productivity of the PGMD desalination system by approximately 17%.

4. Summary and scope for future work

In this section, the reviewed studies are summarized and potential research gaps for future studies on the application of data-driven techniques in the desalination area are also presented. Fig. 4 illustrates the number of reviewed studies in which data-driven methods have been employed across five different applications, including performance prediction using operational parameters, performance prediction using design parameters, optimization and correlation development, maintenance, and control of desalination technologies.

It can be seen from Fig. 4 that investigations on optimization and correlation development of desalination systems have been received more attention compared to the remaining four applications. In this application, the performance of desalination systems was optimized considering operational/design parameters or correlations were developed based on these parameters. It is shown that MD is the most studied desalination method in the optimization or correlation development category having 22 publications, while the SS is in the second rank with 15 publications. Nonetheless, optimization and correlation development of solar-driven MD technologies as a promising environmentally-friendly desalination method has received limited attention and seems a potential future study. A limited number of researchers have also sought to employ data-driven methods for optimization and correlation development in solar-powered HDH desalination systems. It is expected that the use of data-driven optimization techniques by considering both operational and design parameters can play a significant role in enhancing the thermal efficiency and lowering the freshwater cost of these solar-driven desalination systems. Furthermore, Fig. 4 shows that the literature lacks investigations on optimization and correlation development of CDI and ED desalination systems using data-driven tools. Where optimization of CDI desalination method is a complex problem due to joint effect of electrode feature and operational parameters on the salt removal [142,158], application of data-driven optimization techniques such as the RSM method is a promising technique that requires more consideration in the future studies.

Fig. 4 illustrates that the investigations predicting the performance of desalination systems only based on operational parameters ranked second and a vast majority of investigations have been performed on SS and RO desalination systems. Despite a large number of experimental studies on HDH desalination systems in the literature, the development of predictive data-driven models using operational parameters for HDH desalination systems has been received less attention. However, the robustness of various ANN models for the performance prediction of a combined heat pump and HDH desalination system has recently been demonstrated [37]. Likewise, the development of data-driven techniques based on operational parameters for performance prediction of MSF desalination method has been studied only in one investigation [66]. The findings then demonstrated the superiority of the ANN model over the conventional thermodynamic models and conventional experimental correlations for temperature elevation prediction in the MSF desalination system. With respect to the wide application of MSF desalination plants worldwide and therefore data availability, the implementation of ML predictive models can lead to significant energy saving and cost reduction in MSF desalination plants. As shown in Fig. 4, the review of the literature show that a limited number of researchers applied data-driven methods for the performance prediction of CDI desalination process. Due to the dynamic nature of CDI desalination process over the charging period [142], the implementation of the RNN model as an advanced sequential-based predictive model can significantly pave the way for the industrialization of CDI desalination process.

With reference to Fig. 4, compared to investigations on the development of data-driven models based on operational parameters, there are not a significant number of data-driven methods considering design parameters. For instance, design parameters have been taken into account only for developing the data-driven methods in HDH seawater greenhouse systems. However, the application of data-driven methods for analyzing the effects of design parameters on the performance of various HDH configurations has not been investigated yet. Moreover, design parameters have not been considered for performance prediction and optimization of ED, CDI, and MSF desalination systems using data-driven techniques.

Also, a few researchers employed data-driven methods for the maintenance analysis of different desalination systems. Although the literature lacks an accurate modeling tool for wetting prediction in MD desalination systems [150], the application of data-driven methods in this area received insufficient attention. Developing further data-driven

Table 6
Summary of studies on the application of data-driven methods for maintenance purposes.

Ref	Year	System type	Data-driven method	Dataset size/split ratio	Inputs	Outputs	Main remark
[145]	2019	RO	CNN	13,708	• Image	• Fouling growth • Flux decline	• 6000 images were used for training and 4000 images were used for validation and testing the developed CNN model. • A comparison was made between the predictive performance of mathematical methods with the CNN model for fouling modeling. • CNN had better performance than the mathematical methods.
[6]	2021	MD (VMD)	ANN	149	• Time • Feed side temperature • Permeate side pressure • Feed flow rate • Solute concentration in the feed stream	• Permeate flux	• ANN architecture: 5-10-1 • Hyper-parameter tuning method: Trial and Error • Data split: train: 75%, validation: 15%, and test: 15% • Effects of operating parameters on membrane fouling were investigated. • The developed ANN model was coupled with GA optimization method to determine the optimum values of operational parameters. • High membrane fouling happened at higher feed temperatures and lower vacuum pressures. Further, higher feed solute concentrations were also led to higher membrane fouling.
[147]	2008	MD	ANN	229	• Permeate flowrate • Raw water turbidity • Operating time	• Transmembrane pressure drop	• ANN architecture: 3-5-1 • Hyper-parameter tuning method: Trial and Error • A comparison was made between the predictive performance of mathematical (blocking laws) and ANN models for membrane fouling analysis. • ANN showed a great superiority over blocking laws to predict the TMP for all experimental periods.
[148]	2018	RO	ANN	A six-year process database	• Hydraulic parameters (flow rates and pressures) • Water quality parameters (turbidity, total chlorine, and ammonia)	• A new calculated pressure index	• Various hydraulic and water quality parameters (59 parameters) were used to quantify the cause of membrane fouling in a RO system. • A large big dataset was used to assure the validity of the developed model for the first time. • The best predictors of fouling were determined by the aid of ANN. It was shown how the model could be used to reduce fouling rates.
[149]	2020	ED	ANN	22	• Crossflow velocity • Current • Salt concentration	• Stack resistance	• A neural differential equation is fit to experimental data of an ED pilot undergoing humic acid fouling. • It was reported that this model can predict the fouling rate even when using a limited set of experimental data. • It was shown that neural differential equations can extrapolate well to new inputs in simulating colloidal fouling in ED. • By utilizing a Sobol sensitivity analysis, the direct, linear effect of the crossflow velocity is reported as 41% compared to 18.6% and 13.1% for the current and the salt concentration, respectively.
[151]	2020	MD (DCMD)	RSM & ANN	RSM: 31 ANN: 57	• The concentrations of NaCl, CaSO4, alginate and Sodium dodecyl sulfate (SDS)	• Time required to observe the wetting and the maximum recovery of the permeate	• ANN architecture: 4-6-2 • Hyper-parameter tuning method: trial and error • Design method: CCD • Due to the unpredictable behavior of membrane wetting, data-driven methods have been used to predict the wetting phenomena. • Experiments were performed at various concentrations of NaCl, CaSO4, humic acid, alginate, and SDS to examine their effects on the wetting.

(continued on next page)

Table 6 (*continued*)

Ref	Year	System type	Data-driven method	Dataset size/split ratio	Inputs	Outputs	Main remark
[33]	2021	FO	CNN	21 days	• Image	• Fouling characteristics of the membrane (thickness, porosity, roughness, and density of the fouling layer)	• It was shown by data-driven methods that the concentration of NaCl and SDS had the largest effect on the outputs. • The CNN model was successfully developed for fouling prediction. • Thickness, porosity, roughness, and density of the fouling layer were completely analyzed using the CNN method. • Fouling morphology was visualized by real-time optical coherence tomography monitoring. • Dominant fouling characteristics were studied and reported.

models for accurate prediction of the wetting phenomenon in MD modules, particularly for VMD configuration, can lay the foundation for performance enhancement and facilitate the commercialization of this promising technology. Further, it can be inferred from the literature that despite great efforts made by researchers, the fouling phenomenon is still a huge barrier to the industrialization of ED and FO desalination systems [5,19]. Hence, fouling characteristics can be properly analyzed in these desalination technologies with the aid of the CNN deep learning model in which real images are used to develop the model. It is expected this novel fouling analysis method can take big steps in mitigating the fouling issues in membrane-based desalination technologies which deserve more attention in future studies.

It can be also inferred from Fig. 4 that further studies should be carried out on controlling the performance of desalination systems using data-driven methods. Adaptive control of desalination systems with the aid of data-driven techniques can play a key role in performance enhancement and cost reduction of various desalination systems and appears a promising research topic. As shown in Fig. 4, compared to other desalination systems, more investigations have been dedicated to the application of data-driven methods for controlling the performance of the RO system. This can be attributed to the importance of accurate control of industrialized desalination methods such as the RO desalination system. Therefore, the development of advanced controlling tools using data-driven techniques for adaptive control of solar-driven desalination systems such as MD and HDH systems can lay the foundation for the industrialization of these technologies and is a promising future study. By way of illustration, controlling the key operational parameters of HDH desalination system such as the mass ratio of water to air in accordance with the solar radiation intensity seems a viable future study.

Fig. 5 provides information on a breakdown of applied data-driven methods for studying desalination technologies from five different viewpoints. As shown in Fig. 5, among ML models, the ANN method has mostly been applied and researchers placed significant attention on ANN models developed by operational parameters for performance prediction of desalination systems. The statistical methods including TM, RM, FD, and RSM have been mainly employed for optimization and correlation development purposes and the RSM method was the most popular statistical method. Fig. 5 also reveals that DL models have received limited attention despite their vital role in performance enhancement as well as cost reduction of desalination technologies. Hence, the application of RNNs and specifically the LSTM method for adaptive control of solar/wind-driven desalination systems is a promising research potential and requires more extensive attempts. Further, more studies should be carried on assessing the capability of the CNN method to predict complex phenomena such as wetting and fouling issues in membrane-based desalination systems.

The number of times each data-driven method has been applied for analysis of each desalination system is illustrated as a heat map plot in Fig. 6. ANN and RSM methods have received more attention compared to other ML and statistical methods. Researchers also employed the ANN method 20 times for analysis of RO desalination method and the RSM method has been applied 19 times for studying the MD systems. A large area in Fig. 6 is intact indicating no investigation has been conducted which highlights the importance of future studies in these regions. By way of illustration, the classical ML methods including ANFIS, DT, RF, and SVM have not received enough attention. This highlights the direction for future studies on analyzing the performance of these methods compared with the ANN model for investigating different desalination systems. Further studies should also be carried out to compare the performance of classical ML models with conventional thermodynamic and mathematical models in terms of important indicators such as accuracy and computational time. Moreover, Fig. 6 demonstrates that DL methods have been employed only in five investigations. Future studies on the application of DL models as a robust predictor/control tool can facilitate industrialization and decrease the cost of desalination technologies.

Apart from the aforementioned observations, there exist several research points in terms of the effective application of ML methods in desalination systems that require further considerations in future studies. The performance of ML methods is mainly affected by a number of key factors such as appropriate selection of inputs and outputs, concise hyper-parameter tuning, and dataset sizes. In the case of inputs selection, the literature shows that the feature selection analysis has been performed only in a few investigations for the wise inputs selections [75,88,104,142]. Moreover, researchers mainly tended to develop ML models based on operational parameter inputs compared to the design parameters. Regarding outputs, freshwater productivity has been mostly chosen as the output whereas other important outputs such as thermal efficiency, exergy efficiency, and freshwater cost have gained much less attention. With respect to the hyper-parameter tuning method, the findings obtained from our comprehensive literature review revealed that optimization techniques have been applied in a few investigations [77,104,124], and the trial and error method has been widely opted to tune the hyper-parameters. Overall, placing more attention on the mentioned research areas can play a crucial role in increasing the accuracy, generalization capability, as well as lowering the computational time of ML methods. Consequently, this can pave the way for more efficient application of ML models in the desalination region, resulting in performance enhancement and cost reduction of various desalination technologies.

Although collecting a large number of data can be beneficial for data-driven analyses, the data acquisition procedure is often time-consuming and costly. Hence, there should be a trade-off concerning the appropriate number of data for developing accurate data-driven models while taking into account the time and cost of the data collection procedure. To this end, Fig. 7 provides a summary of the whole reviewed papers in terms of the size of the dataset. In Fig. 7, the dataset size with respect to

Table 7
Summary of studies on the application of data-driven methods for control purposes.

Ref	Year	System type	Data-driven method	Dataset size	Inputs	Outputs	Main remark
[34]	2020	RO	RNN (LSTM)	1871	• Feed pressure	• Flow rate of permeate • Permeate concentration	• LSTM model was used as a powerful predictive controller model. • The LSTM predictive model showed a great performance on the validation dataset and was nominated as a robust predictive controller for RO desalination systems.
[152]	2017	RO	ANN	1197	• Power • Temperature • Conductivity	• Pressure • Flow	• ANN architecture for predicting the flow: 3:38:4:1, 3:69:13:1 • ANN architecture for predicting the pressure: 3:56:9:1, 3:71:17:1 • ANNs were used to manage the variable operation of a RO plant. • For the first time the use of ANNs as control system tools for RO units has been studied with a view to enabling a continuous adaptation of the plant's energy consumption to the simulated variable electrical energy generation of a stand-alone wind turbine. • ANNs were able to successfully manage the random and widely varying available electrical power. • The ANN models were used to generate feed flow and operating pressure set points.
[153]	2021	RO	DRL	8760	• One year of load demand • Water demand • Electricity price • Wind turbine output • PV output	• Operating cost • Cost of battery storage system • Pollution cost	• Data split ratio: train: 90% and test: 10% • The energy management of a hybrid energy system is studied as an optimal control objective, and multi-targets are considered along with constraints. • The information entropy theory is used to calculate the weight factor for the trade-off between different targets. Next, a deep reinforcement-learning algorithm is developed to solve this problem and get the optimal control policy. • It was reported that a well-trained agent could provide a better control policy and reduce costs by up to 14.17% compared to other methods.
[154]	2021	SS (stepped)	ANN	n.m.	• n.m.	• n.m.	• Online Sequential Extreme Learning Machine neural network adaptive controller was tested on a stepped SS with $SiO2/TiO2$ nanoparticles in its basin. • Temperature values were stored in a dynamic Binary Search Tree data structure and storage in the memory. • It was concluded that adaptive control of SS process can lead to the optimal cost for the SS with higher performances.
[155]	2013	MD (solar PGMD)	ANN	540	• Feed flow rate	• Distillate flow rate	• ANN architecture: 1-5-1 • Hyper-parameter tuning method: trial and error • Data split: train: 80%, validation: 15%, and test: 5% • A control system based on dynamic ANN was developed to maximize the distillate flow rate. The control system functions based on adjusting the feed flow rate in accordance with variances in solar radiation and temperature of permeate fluid. • The daily productivity was increased by 17.2% with the application of the adaptive control system.
[156]	2015	RO	ANN and GA	474	• Time • Transmembrane pressure • Conductivity • Flow rate	• Permeate flow • Permeate conductivity	• Data split ratio: train: 60%, validation: 20%, and test: 20% • Long-term forecasting and controlling the RO system were studied for the next 5000 h of operation. • By implementing control strategies, permeate conductivity declined for both experimental and model prediction.
[157]	2014	MSF	ANN	4500	• Mass flow rate of the heater vapor • Blow down flow rate • Set point	• Top brine temperature • Level of last stage • Brine salinity	• ANN architecture: 3-12-1 • Hyper-parameter tuning method: Trial and error • Data split: train 75% and test: 25% • Three controllers based on ANN model were considered for controlling the top brine temperature, the level of last stage and salinity. • Results showed that control strategy is viable to be implemented in MSF desalination systems.

the type of desalination system (Fig. 7(a)), and type of data-driven method (Fig. 7(b)) is shown based on various applications: performance prediction using operational parameters, performance prediction using design parameters, optimization and correlation development, maintenance and control. This is evident that a wide range of dataset sizes have been used to develop data-driven methods for analyzing various desalination systems. Among five categories, except for the control category which mainly larger datasets have been used (with minimum and mean of 474 and 3497, respectively), data-driven models exhibited appropriate accuracy in the other four groups with less than 500 data. Furthermore, according to Fig. 7(a), a broad spectrum of data has been used for MD and RO desalination systems compared to other desalination systems. Regarding data-driven models as shown in Fig. 7(b), the ANN model developed by less than 500 data is the most popular ML method. Moreover, statistical methods including TM, RM, FD, and RSM methods are generally applied using small-sized datasets, with maximum 200 data. The largest dataset size (13708) can be also seen in terms of the application of the CNN model for studying maintenance in the RO desalination system. Overall, Fig. 7 reveals that a wide range of dataset sizes have been applied in various data-driven methods for the

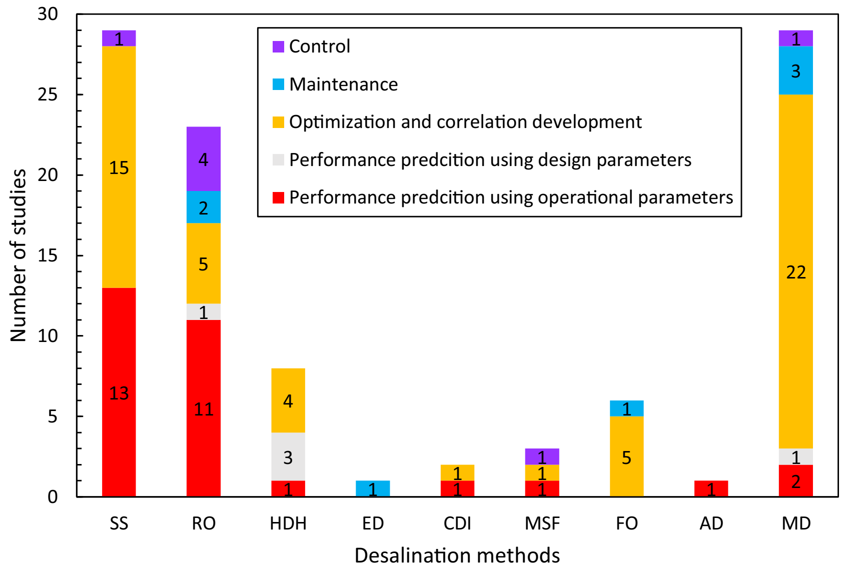

Fig. 4. The number of reviewed studies versus desalination systems for different applications.

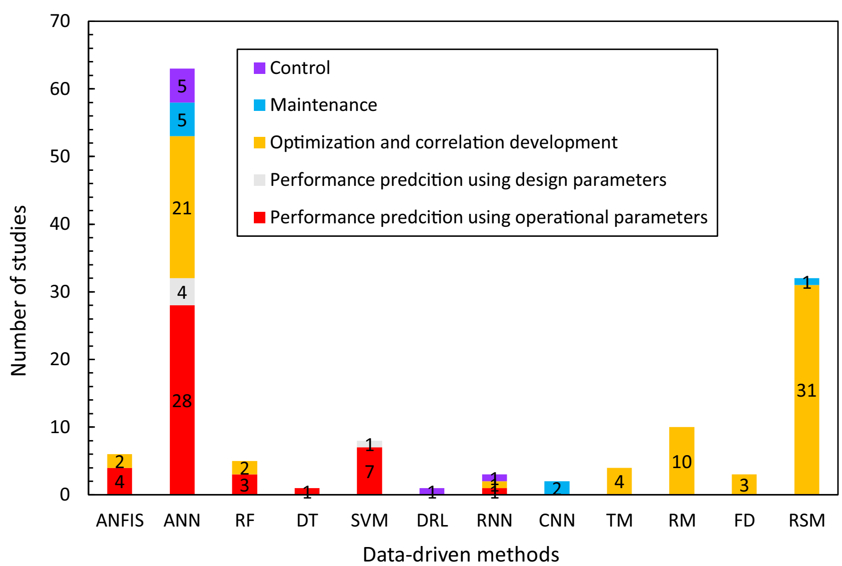

Fig. 5. The number of reviewed studies versus data-driven methods for different applications.

analysis of different desalination systems. Therefore, the accuracy of data-driven methods developed by a different number of data should be investigated in future studies that can lead to a significant saving on time and cost of the data acquisition procedure.

5. Conclusions

This paper comprehensively reviewed the application of data-driven methods (both AI and DOE methods) in thermal and membrane desalination systems. The reviewed studies have been thoroughly categorized based on the type of desalination system, type of data-driven method, and the application of data-driven methods for the analysis of various desalination systems. The literature review showed that data-driven methods have been mainly applied for the analysis of desalination systems for five different applications namely performance prediction using operational parameters, performance prediction considering design parameters, optimization and correlation development, maintenance, and control. Compared to the complexity involved in mathematical modeling of desalination systems, data-driven methods exhibited great performance with much lower complexity and maintaining high accuracy. However, a review of a large number of investigations indicated that despite great efforts made by researchers, there are extensive unexplored and potential research areas concerning the data-driven analysis of desalination technologies. The following main conclusions can be drawn from the current review:

- Regarding membrane-based desalination systems, a vast majority of studies were carried out on RO and MD desalination systems. However, there are several unexplored research areas in terms of the application of data-driven techniques for control and maintenance analysis of these systems, including adaptive control of solar-driven MD system, adaptive control of wind-powered RO technology, and fouling/wetting analysis in MD desalination systems. Further, the review of literature reveals that data-driven methods can play a key role in performance prediction, optimization, and maintenance analysis of CDI, ED, and FO desalination systems. More data-driven

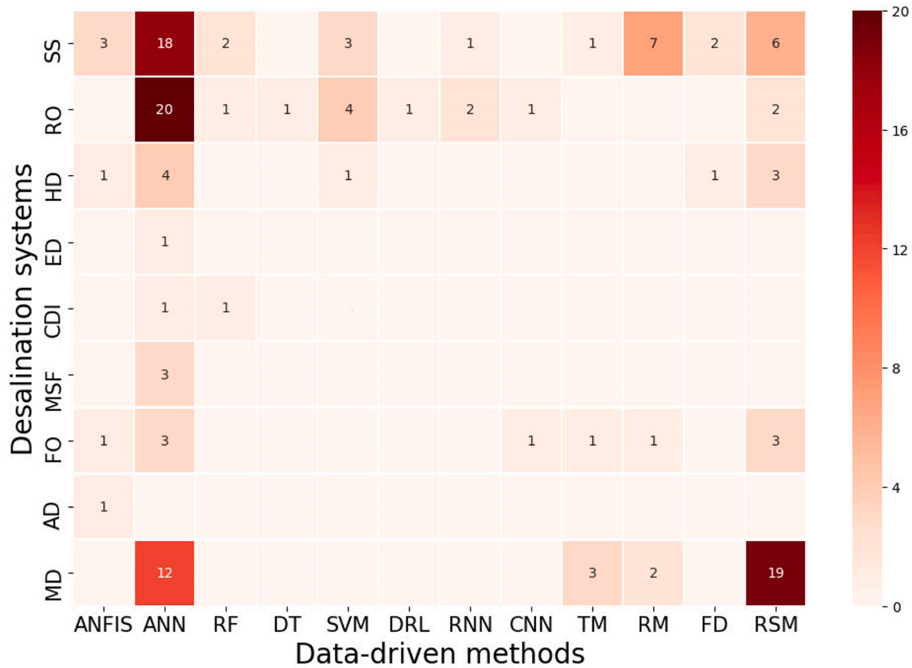

Fig. 6. Heat map illustration of applied data-driven methods in different desalination systems.

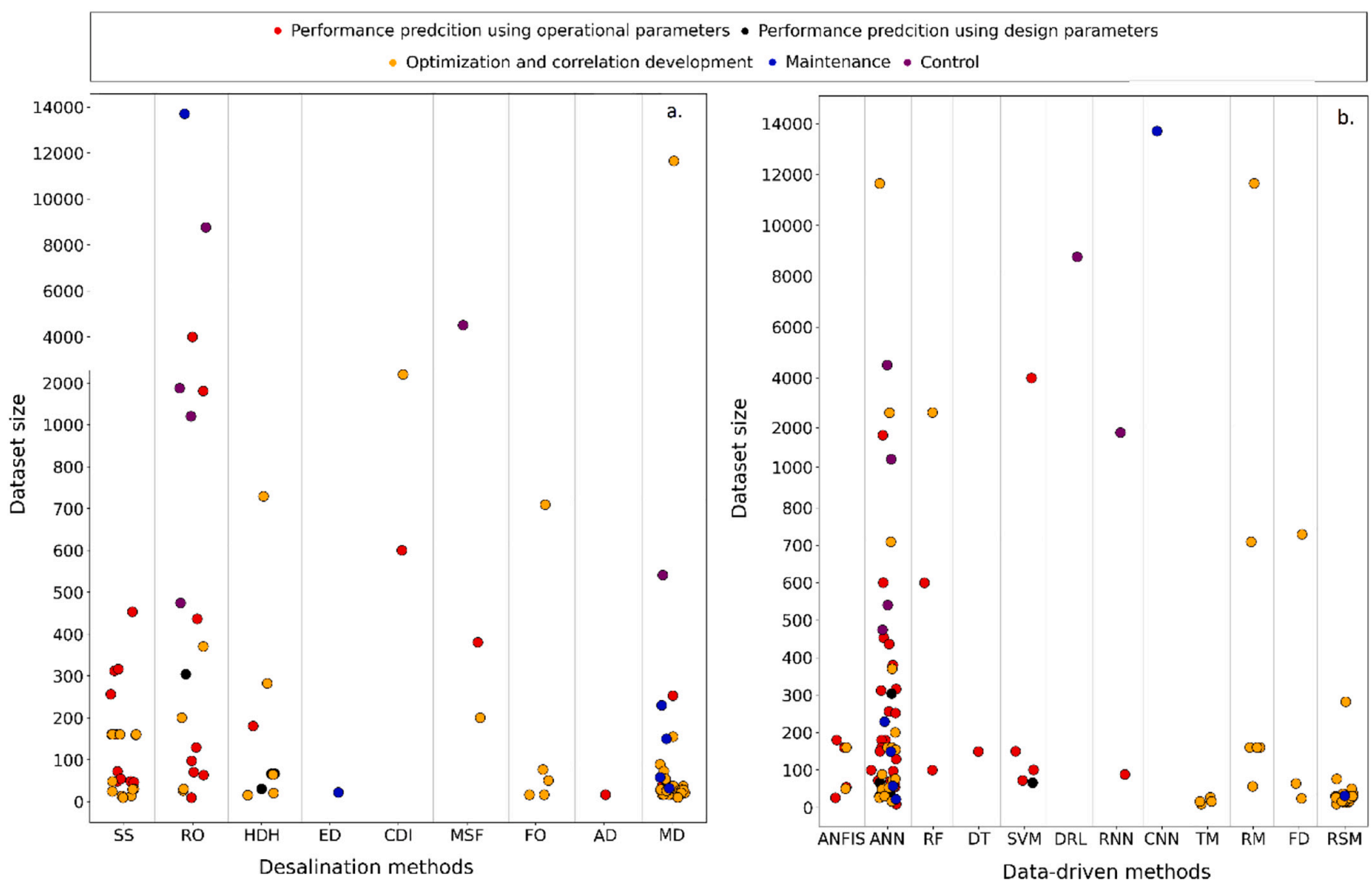

Fig. 7. Size of datasets with respect to (a) desalination systems and (b) data-driven methods for different applications.

investigations should be conducted on performance analysis and optimization of CDI systems considering the combined effect of operational and electrode features. Furthermore, image processing using the CNN deep learning model can significantly facilitate fouling diagnosis in ED and FO desalination technologies.

- With respect to thermal desalination systems, researchers mostly applied data-driven methods to analyze the SS desalination system.

However, AD technology as a novel desalination method has not been studied sufficiently via data-driven approaches. A limited number of investigations conducted on HDH and MSF desalination technologies proved the enhanced predictive performance of ML models compared to mathematical models and experimental correlations. Nonetheless, this review paper showed that other applications of data-driven methods for in-depth analysis of HDH and MSF systems require more attention, including performance prediction based on both operational and design parameters, and control of solar-driven systems.

- In the case of data-driven methods, it can be concluded that among ML and DOE methods, ANN and RSM were the most popular methods, respectively. Moreover, the results reported by a few investigations prove the robustness of other ML methods such as ANFIS, SVM, and RF methods for accurate analysis of desalination systems, which highlights performing more studies on developing other classical ML methods for the analysis of different desalination technologies. Further, a limited number of investigations performed on the application of DL models in the desalination area confirmed the reliability of DL models for accurate analysis of desalination technologies. It appears that DL models have the potential to open new research directions in terms of different applications in thermal and membrane desalination systems, including prediction of the dynamic behavior of desalination systems, maintenance analysis of membrane-based systems, and adaptive control of renewable-based desalination systems.
- Compared to operational parameters, design parameters have received insufficient attention for developing data-driven methods. Furthermore, freshwater productivity was frequently chosen as the output of data-driven models, and other important outputs such as energy and exergy efficiencies and freshwater cost should be given more attention.
- The review of literature from the dataset size viewpoint shows that analyzing the effect of dataset sizes on the performance of data-driven methods can pave the path for lowering the cost and time of the data collection.
- It is expected that data-driven methods can play a vital role in overcoming the obstacles to the industrialization of several desalination systems such as HDH, CDI, AD, ED, MD, and FO technologies. Further, ML and DL methods can be effectively employed for in-depth analysis of industrialized desalination technologies, resulting in performance enhancement and cost reduction.

Declaration of competing interest

We wish to confirm that there are no known conflicts of interest associated with this publication and there has been no significant financial support for this work that could have influenced its outcome.

References

[1] U. Water, 2018 UN World Water Development Report, Nature-based Solutions for Water, 2018.
[2] M.A.E.-R. Abu-Zeid, Y. Zhang, H. Dong, L. Zhang, H.-L. Chen, L. Hou, A comprehensive review of vacuum membrane distillation technique, Desalination 356 (2015) 1–14.
[3] M. Faegh, P. Behnam, M.B. Shafii, A review on recent advances in humidification-dehumidification (HDH) desalination systems integrated with refrigeration, power and desalination technologies, Energy Convers. Manag. 196 (2019) 1002–1036.
[4] M.R. Rahimpour, N.M. Kazerooni, M. Parhoudeh, Water treatment by renewable energy-driven membrane distillation, in: Current Trends and Future Developments on (Bio-) Membranes, Elsevier, 2019, pp. 179–211.
[5] S.K. Singh, C. Sharma, A. Maiti, A comprehensive review of standalone and hybrid forward osmosis for water treatment: membranes and recovery strategies of draw solutions, J. Environ. Chem. Eng. (2021) 105473.
[6] S. Mittal, A. Gupta, S. Srivastava, M. Jain, Artificial neural network based modeling of the vacuum membrane distillation process: effects of operating parameters on membrane fouling, Chem. Eng. Process. Process Intensif. 164 (2021), 108403.
[7] S. Al Aani, T. Bonny, S.W. Hasan, N. Hilal, Can machine language and artificial intelligence revolutionize process automation for water treatment and desalination? Desalination 458 (2019) 84–96.
[8] R. Mahadevaa, G. Manika, A. Goela, N. Dhakalb, A review of the artificial neural network based modelling and simulation approaches applied to optimize reverse osmosis desalination techniques, Desalin. Water Treat. 156 (2019) 245–256.
[9] M. Asghari, A. Dashti, M. Rezakazemi, E. Jokar, H. Halakoei, Application of neural networks in membrane separation, Rev. Chem. Eng. 36 (2) (2020) 265–310.
[10] J. Jawad, A.H. Hawari, S.J. Zaidi, Artificial neural network modeling of wastewater treatment and desalination using membrane processes: a review, Chem. Eng. J. 419 (2021), 129540.
[11] M.Alhuyi Nazari, M. Salem, I. Mahariq, K. Younes, B. Maqableh, Utilization of data-driven methods in solar desalination systems: a comprehensive review, Front. Energy Res 9 (2021) 742615.
[12] E.J. Okampo, N. Nwulu, Optimisation of renewable energy powered reverse osmosis desalination systems: a state-of-the-art review, Renew. Sust. Energ. Rev. 140 (2021), 110712.
[13] K. Park, J. Kim, D.R. Yang, S. Hong, Towards a low-energy seawater reverse osmosis desalination plant: a review and theoretical analysis for future directions, J. Membr. Sci. 595 (2020), 117607.
[14] M. Khayet, C. Cojocaru, M. Essalhi, Artificial neural network modeling and response surface methodology of desalination by reverse osmosis, J. Membr. Sci. 368 (1–2) (2011) 202–214.
[15] P.M. Pardeshi, A.A. Mungray, A.K. Mungray, Determination of optimum conditions in forward osmosis using a combined Taguchi–neural approach, Chem. Eng. Res. Des. 109 (2016) 215–225.
[16] J. Jawad, A.H. Hawari, S.J. Zaidi, Modeling and sensitivity analysis of the forward osmosis process to predict membrane flux using a novel combination of neural network and response surface methodology techniques, Membranes 11 (1) (2021) 70.
[17] D. González, J. Amigo, F. Suárez, Membrane distillation: perspectives for sustainable and improved desalination, Renew. Sust. Energ. Rev. 80 (2017) 238–259.
[18] A. Anvari, A. Azimi Yancheshme, K.M. Kekre, A. Ronen, State-of-the-art methods for overcoming temperature polarization in membrane distillation process: a review, J. Membr. Sci. 616 (2020), 118413.
[19] S. Al-Amshawee, M.Y.B.M. Yunus, A.A.M. Azoddein, D.G. Hassell, I.H. Dakhil, H. A. Hasan, Electrodialysis desalination for water and wastewater: a review, Chem. Eng. J. 380 (2020), 122231.
[20] L. Karimi, A. Ghassemi, How operational parameters and membrane characteristics affect the performance of electrodialysis reversal desalination systems: the state of the art, J. Membr. Sci. Res. 2 (3) (2016) 111–117.
[21] M. Suss, S. Porada, X. Sun, P. Biesheuvel, J. Yoon, V. Presser, Water desalination via capacitive deionization: what is it and what can we expect from it? Energy Environ. Sci. 8 (8) (2015) 2296–2319.
[22] V.P. Katekar, S.S. Deshmukh, Techno-economic review of solar distillation systems: a closer look at the recent developments for commercialisation, J. Clean. Prod. 294 (2021), 126289.
[23] G.P. Narayan, M.H. Sharqawy, J.H. Lienhard V, S.M. Zubair, Thermodynamic analysis of humidification dehumidification desalination cycles, Desalin. Water Treat. 16 (1-3) (2010) 339–353.
[24] D.U. Lawal, N.A. Qasem, Humidification-dehumidification desalination systems driven by thermal-based renewable and low-grade energy sources: a critical review, Renew. Sust. Energ. Rev. 125 (2020), 109817.
[25] F.A. Essa, A.S. Abdullah, Z.M. Omara, A.E. Kabeel, W.M. El-Maghlany, On the different packing materials of humidification–dehumidification thermal desalination techniques – a review, J. Clean. Prod. 277 (2020), 123468.
[26] M. Prajapati, M. Shah, B. Soni, A review of geothermal integrated desalination: a sustainable solution to overcome potential freshwater shortages, J. Clean. Prod. 326 (2021), 129412.
[27] H. Baig, M.A. Antar, S.M. Zubair, Performance characteristics of a once-through multi-stage flash distillation process, Desalin. Water Treat. 13 (1–3) (2010) 174–185.
[28] K. Sztekler, et al., Experimental study of three-bed adsorption chiller with desalination function, Energies 13 (21) (2020) 5827.
[29] K. Sztekler, et al., Performance evaluation of a single-stage two-bed adsorption chiller with desalination function, J. Energy Resour. Technol. 143 (8) (2021).
[30] A.H. Elsheikh, S.W. Sharshir, M. Abd Elaziz, A. Kabeel, W. Guilan, Z. Haiou, Modeling of solar energy systems using artificial neural network: a comprehensive review, Sol. Energy 180 (2019) 622–639.
[31] K.S. Garud, S. Jayaraj, M.Y. Lee, A review on modeling of solar photovoltaic systems using artificial neural networks, fuzzy logic, genetic algorithm and hybrid models, Int. J. Energy Res. 45 (1) (2021) 6–35.
[32] P. Behnam, M. Faegh, M.B. Shafii, M. Khiadani, A comparative study of various machine learning methods for performance prediction of an evaporative condenser, Int. J. Refrig. 126 (2021) 280–290.
[33] S.J. Im, N.D. Viet, A. Jang, Real-time monitoring of forward osmosis membrane fouling in wastewater reuse process performed with a deep learning model, Chemosphere 275 (2021), 130047.
[34] D. Karimanzira, T. Rauschenbach, Deep learning based model predictive control for a reverse osmosis desalination plant, J. Appl. Math. Phys. 8 (12) (2020) 2713–2731.
[35] M. Mäkelä, Experimental design and response surface methodology in energy applications: a tutorial review, Energy Convers. Manag. 151 (2017) 630–640.

[36] H.K. Ghritlahre, R.K. Prasad, Application of ANN technique to predict the performance of solar collector systems-a review, Renew. Sust. Energ. Rev. 84 (2018) 75–88.
[37] M. Faegh, P. Behnam, M.B. Shafii, M. Khiadani, Development of artificial neural networks for performance prediction of a heat pump assisted humidification-dehumidification desalination system, Desalination 508 (2021), 115052.
[38] L. Khaouane, Y. Ammi, S. Hanini, Modeling the retention of organic compounds by nanofiltration and reverse osmosis membranes using bootstrap aggregated neural networks, Arab. J. Sci. Eng. 42 (4) (2017) 1443–1453.
[39] M. Hamdan, H.R. Khalil, E. Abdelhafez, Comparison of neural network models in the estimation of the performance of solar still under Jordanian climate, J. Clean Energy Technol. 1 (3) (2013) 238–242.
[40] F. Essa, M. Abd Elaziz, A.H. Elsheikh, Prediction of power consumption and water productivity of seawater greenhouse system using random vector functional link network integrated with artificial ecosystem-based optimization, Process Saf. Environ. Prot. 144 (2020) 322–329.
[41] D. Husmeier, Random vector functional link (RVFL) networks, in: D. Husmeier (Ed.), Neural Networks for Conditional Probability Estimation: Forecasting Beyond Point Predictions, Springer London, London, 1999, pp. 87–97.
[42] S. Sapna, A. Tamilarasi, M.P. Kumar, Backpropagation learning algorithm based on levenberg marquardt algorithm, Comp. Sci. Inform. Technol. (CS and IT) 2 (2012) 393–398.
[43] E. Atashpaz-Gargari, C. Lucas, Imperialist competitive algorithm: an algorithm for optimization inspired by imperialistic competition, in: 2007 IEEE Congress on Evolutionary Computation, Ieee, 2007, pp. 4661–4667.
[44] S. Mirjalili, J. Song Dong, A.S. Sadiq, H. Faris, Genetic algorithm: theory, literature review, and application in image reconstruction, in: S. Mirjalili, J. Song Dong, A. Lewis (Eds.), Nature-inspired Optimizers: Theories, Literature Reviews and Applications, Springer International Publishing, Cham, 2020, pp. 69–85.
[45] Q.H. Nguyen, et al., A novel hybrid model based on a feedforward neural network and one step secant algorithm for prediction of load-bearing capacity of rectangular concrete-filled steel tube columns, Molecules 25 (15) (2020).
[46] H.B. Demuth, M.H. Beale, O.De Jess, M.T. Hagan, Neural Network Design, Martin Hagan, 2014.
[47] A.D. Anastasiadis, G.D. Magoulas, M.N. Vrahatis, New globally convergent training scheme based on the resilient propagation algorithm, Neurocomputing 64 (2005) 253–270.
[48] R. Rojas, Neural Networks: A Systematic Introduction, Springer Science & Business Media, 2013.
[49] R. Fletcher, Practical Methods of Optimization, John Wiley & Sons, 2013.
[50] J. Mockus, Bayesian approach to global optimization: theory and applications, Springer Science & Business Media, 2012.
[51] H. Sayyaadi, Chapter 8 - real-time optimization of energy systems using the soft-computing approaches, in: H. Sayyaadi (Ed.), Modeling, Assessment, and Optimization of Energy Systems, Academic Press, 2021, pp. 479–527.
[52] A. Géron, Hands-on Machine Learning With Scikit-Learn, Keras, and TensorFlow: Concepts, Tools, and Techniques to Build Intelligent Systems, O'Reilly Media, 2019.
[53] M.W. Ahmad, J. Reynolds, Y. Rezgui, Predictive modelling for solar thermal energy systems: a comparison of support vector regression, random forest, extra trees and regression trees, J. Clean. Prod. 203 (2018) 810–821.
[54] D. Maulud, A.M. Abdulazeez, A review on linear regression comprehensive in machine learning, J. Appl. Sci. Technol. Trends 1 (4) (2020) 140–147.
[55] R.R. Hocking, Methods and Applications of Linear Models: Regression and the Analysis of Variance, John Wiley & Sons, 2013.
[56] S. Aslam, H. Herodotou, S.M. Mohsin, N. Javaid, N. Ashraf, S. Aslam, A survey on deep learning methods for power load and renewable energy forecasting in smart microgrids, Renew. Sust. Energ. Rev. 144 (2021), 110992.
[57] P. Garnier, J. Viquerat, J. Rabault, A. Larcher, A. Kuhnle, E. Hachem, A review on deep reinforcement learning for fluid mechanics, Comput. Fluids 225 (2021), 104973.
[58] S.T. Bouguecha, A. Boubakri, S.E. Aly, M.H. Al-Beirutty, M.M. Hamdi, Optimization of permeate flux produced by solar energy driven membrane distillation process using central composite design approach, Water Sci. Technol. 74 (1) (2016) 87–98.
[59] A.E. Khalifa, D.U. Lawal, Application of response surface and taguchi optimization techniques to air gap membrane distillation for water desalination—a comparative study, Desalin. Water Treat. 57 (59) (2016) 28513–28530.
[60] M. Akbari, P. Asadi, M.K.Besharati Givi, G. Khodabandehlouie, 13 - Artificial neural network and optimization, in: M.K.B. Givi, P. Asadi (Eds.), Advances in Friction-Stir Welding and Processing, Woodhead Publishing, 2014, pp. 543–599.
[61] J. Antony, 6 - full factorial designs, in: J. Antony (Ed.), Design of Experiments for Engineers and Scientists, Second Edition, Elsevier, Oxford, 2014, pp. 63–85.
[62] J. Antony, 7 - Fractional factorial designs, in: J. Antony (Ed.), Design of Experiments for Engineers and Scientists, Second Edition, Elsevier, Oxford, 2014, pp. 87–112.
[63] R. Chauhan, P. Dumka, D.R. Mishra, Modelling conventional and solar earth still by using the LM algorithm-based artificial neural network, Int. J. Ambient Energy (2020) 1–8.
[64] A. Bagheri, N. Esfandiari, B. Honarvar, A. Azdarpour, First principles versus artificial neural network modelling of a solar desalination system with experimental validation, Math. Comput. Model. Dyn. Syst. 26 (5) (2020) 453–480.
[65] A.M. Aish, H.A. Zaqoot, S.M. Abdeljawad, Artificial neural network approach for predicting reverse osmosis desalination plants performance in the Gaza strip, Desalination 367 (2015) 240–247.
[66] A. Aminian, Prediction of temperature elevation for seawater in multi-stage flash desalination plants using radial basis function neural network, Chem. Eng. J. 162 (2) (2010) 552–556.
[67] M. Bahiraei, S. Nazari, H. Moayedi, H. Safarzadeh, Using neural network optimized by imperialist competition method and genetic algorithm to predict water productivity of a nanofluid-based solar still equipped with thermoelectric modules, Powder Technol. 366 (2020) 571–586.
[68] E. Salami, M. Ehetshami, A. Karimi-Jashni, M. Salari, S.N. Sheibani, A. Ehteshami, A mathematical method and artificial neural network modeling to simulate osmosis membrane's performance, Model. Earth Syst. Environ. 2 (4) (2016) 1–11.
[69] A. Salgado-Reyna, et al., Artificial neural networks for modeling the reverse osmosis unit in a wastewater pilot treatment plant, Desalin. Water Treat. 53 (5) (2015) 1177–1187.
[70] A. Abbas, N. Al-Bastaki, Modeling of an RO water desalination unit using neural networks, Chem. Eng. J. 114 (1–3) (2005) 139–143.
[71] A.T. Mohammad, M.A. Al-Obaidi, E.M. Hameed, B.N. Basheer, I.M. Mujtaba, Modelling the chlorophenol removal from wastewater via reverse osmosis process using a multilayer artificial neural network with genetic algorithm, J. Water Process Eng. 33 (2020), 100993.
[72] M.I. Kizhisseri, M.M. Mohamed, M.A. Hamouda, Prediction of capital cost of ro based desalination plants using machine learning approach, in: E3S Web of Conferences 158, EDP Sciences, 2020, p. 06001.
[73] A.F. Mashaly, A. Alazba, Comparative investigation of artificial neural network learning algorithms for modeling solar still production, J. Water Reuse Desalin. 5 (4) (2015) 480–493.
[74] R. Chauhan, S. Sharma, R. Pachauri, P. Dumka, D.R. Mishra, Experimental and theoretical evaluation of thermophysical properties for moist air within solar still by using different algorithms of artificial neural network, J. Energy Storage 30 (2020), 101408.
[75] N.I. Santos, A.M. Said, D.E. James, N.H. Venkatesh, Modeling solar still production using local weather data and artificial neural networks, Renew. Energy 40 (1) (2012) 71–79.
[76] A.F. Mashaly, A. Alazba, A. Al-Awaadh, M.A. Mattar, Predictive model for assessing and optimizing solar still performance using artificial neural network under hyper arid environment, Sol. Energy 118 (2015) 41–58.
[77] M. Tavakolmoghadam, M. Safavi, An optimized neural network model of desalination by vacuum membrane distillation using genetic algorithm, Procedia Eng. 42 (2012) 106–112.
[78] W. Cao, Q. Liu, Y. Wang, I.M. Mujtaba, Modeling and simulation of VMD desalination process by ANN, Comput. Chem. Eng. 84 (2016) 96–103.
[79] X. Pascual, et al., Data-driven models of steady state and transient operations of spiral-wound RO plant, Desalination 316 (2013) 154–161.
[80] M. Bahiraei, S. Nazari, H. Safarzadeh, Modeling of energy efficiency for a solar still fitted with thermoelectric modules by ANFIS and PSO-enhanced neural network: a nanofluid application, Powder Technol. 385 (2021) 185–198.
[81] A.F. Mashaly, A. Alazba, Application of adaptive neuro-fuzzy inference system (ANFIS) for modeling solar still productivity, J. Water Supply Res. Technol.—AQUA 66 (6) (2017) 367–380.
[82] P. Cabrera, J.A. Carta, J. Gonzalez, G. Melian, Wind-driven SWRO desalination prototype with and without batteries: a performance simulation using machine learning models, Desalination 435 (2018) 77–96.
[83] F.A. Essa, M. Abd Elaziz, A.H. Elsheikh, An enhanced productivity prediction model of active solar still using artificial neural network and Harris hawks optimizer, Appl. Therm. Eng. 170 (2020), 115020.
[84] A. Sohani, S. Hoseinzadeh, S. Samiezadeh, I. Verhaert, Machine learning prediction approach for dynamic performance modeling of an enhanced solar still desalination system, J. Therm. Anal. Calorim. (2021) 1–12.
[85] A.H. Elsheikh, V.P. Katekar, O.L. Muskens, S.S. Deshmukh, M. Abd Elaziz, S. M. Dabour, Utilization of LSTM neural network for water production forecasting of a stepped solar still with a corrugated absorber plate, Process Saf. Environ. Prot. 148 (2021) 273–282.
[86] M. Ehteram, S.Q. Salih, Z.M. Yaseen, Efficiency evaluation of reverse osmosis desalination plant using hybridized multilayer perceptron with particle swarm optimization, Environ. Sci. Pollut. Res. (2020) 1–14.
[87] D. Libotean, J. Giralt, F. Giralt, R. Rallo, T. Wolfe, Y. Cohen, Neural network approach for modeling the performance of reverse osmosis membrane desalting, J. Membr. Sci. 326 (2) (2009) 408–419.
[88] F. Saffarimiandoab, R. Mattesini, W. Fu, E.E. Kuruoglu, X. Zhang, Interpretable machine learning modeling of capacitive deionization for contribution analysis of electrode and process features, J. Mater. Chem. A 9 (4) (2021) 2259–2268.
[89] H. Alhumade, H. Rezk, A.A. Al-Zahrani, S.F. Zaman, A. Askalany, Artificial intelligence based modelling of adsorption water desalination system, Mathematics 9 (14) (2021) 1674.
[90] A.W. Kandeal, et al., Productivity modeling enhancement of a solar desalination unit with nanofluids using machine learning algorithms integrated with bayesian optimization, Energy Technol. 9 (9) (2021) 2100189.
[91] F. Iranmanesh, A. Moradi, M. Rafizadeh, Implementation of radial basic function networks for the prediction of RO membrane performances by using a complex transport model, Desalin. Water Treat. 57 (43) (2016) 20307–20317.
[92] T. Zarei, R. Behyad, Predicting the water production of a solar seawater greenhouse desalination unit using multi-layer perceptron model, Sol. Energy 177 (2019) 595–603.

[93] T. Zarei, R. Behyad, E. Abedini, Study on parameters effective on the performance of a humidification-dehumidification seawater greenhouse using support vector regression, Desalination 435 (2018) 235–245.
[94] C. Yang, et al., Prediction model to analyze the performance of VMD desalination process, Comput. Chem. Eng. 132 (2020), 106619.
[95] M.O. Abu Abbas, M.Y. Al-Abed Allah, Q.N. Al-Oweiti, Optimization analysis of active solar still using design of experiment method, in: Drinking Water Engineering and Science Discussions, 2020, pp. 1–24.
[96] O. Rejeb, M.S. Yousef, C. Ghenai, H. Hassan, M. Bettayeb, Investigation of a solar still behaviour using response surface methodology, Case Stud. Therm. Eng. 24 (2021), 100816.
[97] D. Cheng, W. Gong, N. Li, Response surface modeling and optimization of direct contact membrane distillation for water desalination, Desalination 394 (2016) 108–122.
[98] D. Cheng, et al., Simulation and multi-objective optimization of heat and mass transfer in direct contact membrane distillation by response surface methodology integrated modeling, Chem. Eng. Res. Des. 159 (2020) 565–581.
[99] D. Cheng, N. Li, J. Zhang, Modeling and multi-objective optimization of vacuum membrane distillation for enhancement of water productivity and thermal efficiency in desalination, Chem. Eng. Res. Des. 132 (2018) 697–713.
[100] J.D. Gil, A. Ruiz-Aguirre, L. Roca, G. Zaragoza, M. Berenguel, Prediction models to analyse the performance of a commercial-scale membrane distillation unit for desalting brines from RO plants, Desalination 445 (2018) 15–28.
[101] A.F. Mashaly, A. Alazba, Artificial intelligence for predicting solar still production and comparison with stepwise regression under arid climate, J. Water Supply Res. Technol. AQUA 66 (3) (2017) 166–177.
[102] A.F. Mashaly, A. Alazba, Assessing the accuracy of ANN, ANFIS, and MR techniques in forecasting productivity of an inclined passive solar still in a hot, arid environment, Water SA 45 (2) (2019) 239–250.
[103] A.F. Mashaly, A. Alazba, Comparison of ANN, MVR, and SWR models for computing thermal efficiency of a solar still, Int. J. Green Energy 13 (10) (2016) 1016–1025.
[104] Y. Wang, et al., Prediction of tubular solar still performance by machine learning integrated with bayesian optimization algorithm, Appl. Therm. Eng. 184 (2021), 116233.
[105] A.F. Mashaly, A. Alazba, Thermal performance analysis of an inclined passive solar still using agricultural drainage water and artificial neural network in arid climate, Sol. Energy 153 (2017) 383–395.
[106] L. Acevedo, J. Uche, A. Del-Amo, Improving the distillate prediction of a membrane distillation unit in a trigeneration scheme by using artificial neural networks, Water 10 (3) (2018) 310.
[107] Z. Rahimi-Ahar, M.S. Hatamipour, Y. Ghalavand, Experimental investigation of a solar vacuum humidification-dehumidification (VHDH) desalination system, Desalination 437 (2018) 73–80.
[108] Z. Rahimi-Ahar, M.S. Hatamipour, Performance evaluation of a solar and vacuum assisted multi-stage humidification-dehumidification desalination system, Process Saf. Environ. Prot. 148 (2021/04/01/ 2021.) 1304–1314.
[109] S. Farsad, A. Behzadmehr, Analysis of a solar desalination unit with humidification–dehumidification cycle using DoE method, Desalination 278 (1–3) (2011) 70–76.
[110] V. Okati, A. Behzadmehr, S. Farsad, Analysis of a solar desalinator (humidification–dehumidification cycle) including a compound system consisting of a solar humidifier and subsurface condenser using DoE, Desalination 397 (2016) 9–21.
[111] S. Rashidi, M. Bovand, J.A. Esfahani, Optimization of partitioning inside a single slope solar still for performance improvement, Desalination 395 (2016) 79–91.
[112] S. Rashidi, M. Bovand, N. Rahbar, J.A. Esfahani, Steps optimization and productivity enhancement in a nanofluid cascade solar still, Renew. Energy 118 (2018) 536–545.
[113] Y.G. Lee, et al., Artificial neural network model for optimizing operation of a seawater reverse osmosis desalination plant, Desalination 247 (1–3) (2009) 180–189.
[114] Q. Li, J. Loy-Benitez, K. Nam, S. Hwangbo, J. Rashidi, C. Yoo, Sustainable and reliable design of reverse osmosis desalination with hybrid renewable energy systems through supply chain forecasting using recurrent neural networks, Energy 178 (2019) 277–292.
[115] M. Barello, D. Manca, R. Patel, I.M. Mujtaba, Neural network based correlation for estimating water permeability constant in RO desalination process under fouling, Desalination 345 (2014) 101–111.
[116] A. Srivastava, et al., Response surface methodology and artificial neural network modelling for the performance evaluation of pilot-scale hybrid nanofiltration (NF) & reverse osmosis (RO) membrane system for the treatment of brackish ground water, J. Environ. Manag. 278 (2021), 111497.
[117] K. Aghilesh, A. Mungray, S. Agarwal, J. Ali, M.C. Garg, Performance optimisation of forward-osmosis membrane system using machine learning for the treatment of textile industry wastewater, J. Clean. Prod. 289 (2021), 125690.
[118] M. Khayet, J. Sanmartino, M. Essalhi, M. García-Payo, N. Hilal, Modeling and optimization of a solar forward osmosis pilot plant by response surface methodology, Sol. Energy 137 (2016) 290–302.
[119] J. Jawad, A.H. Hawari, S. Zaidi, Modeling of forward osmosis process using artificial neural networks (ANN) to predict the permeate flux, Desalination 484 (2020), 114427.
[120] S.J.P. Gnanaraj, V. Velmurugan, An experimental investigation to optimize the production of single and stepped basin solar stills-a Taguchi approach, Energy Sources, Part A (2020) 1–24.
[121] A. Senthil Rajan, K. Raja, P. Marimuthu, Increasing the productivity of pyramid solar still augmented with biomass heat source and analytical validation using RSM, Desalin. Water Treat. 57 (10) (2016) 4406–4419.
[122] S. Nazari, M. Bahiraei, H. Moayedi, H. Safarzadeh, A proper model to predict energy efficiency, exergy efficiency, and water productivity of a solar still via optimized neural network, J. Clean. Prod. 277 (2020), 123232.
[123] R. Prasad, D. Singh, A. Sharma, An experimental and statistical analysis of double slope single basin solar still in active and passive mode with different water depth, IOP Conference Series: Materials Science and Engineering 691 (1) (2019) 012090. IOP Publishing.
[124] M.S.S. Abujazar, S. Fatihah, I.A. Ibrahim, A. Kabeel, S. Sharil, Productivity modelling of a developed inclined stepped solar still system based on actual performance and using a cascaded forward neural network model, J. Clean. Prod. 170 (2018) 147–159.
[125] O. Haitham, M. Jamel, S. Ihab, Statistical analysis and mathematical modeling of modified single slope solar still, Energy Sources, Part A (2020) 1–19.
[126] L.D. Jathar, S. Ganesan, Statistical analysis of brick, sand and concrete pieces on the performance of concave type stepped solar still, Int. J. Ambient Energy (2020) 1–17.
[127] Q. He, P. Li, H. Geng, C. Zhang, J. Wang, H. Chang, Modeling and optimization of air gap membrane distillation system for desalination, Desalination 354 (2014) 68–75.
[128] V.T. Shahu, S. Thombre, Analysis and optimization of a new cylindrical air gap membrane distillation system, Water Supply 20 (1) (2020) 361–371.
[129] M. Khayet, C. Cojocaru, C. García-Payo, Application of response surface methodology and experimental design in direct contact membrane distillation, Ind. Eng. Chem. Res. 46 (17) (2007) 5673–5685.
[130] A. Ruiz-Aguirre, J.A. Andrés-Mañas, J.M. Fernández-Sevilla, G. Zaragoza, Experimental characterization and optimization of multi-channel spiral wound air gap membrane distillation modules for seawater desalination, Sep. Purif. Technol. 205 (2018) 212–222.
[131] A. Ruiz-Aguirre, J.A. Andrés-Mañas, J.M. Fernández-Sevilla, G. Zaragoza, Modeling and optimization of a commercial permeate gap spiral wound membrane distillation module for seawater desalination, Desalination 419 (2017) 160–168.
[132] M. Khayet, C. Cojocaru, A. Baroudi, Modeling and optimization of sweeping gas membrane distillation, Desalination 287 (2012/02/15/ 2012.) 159–166.
[133] M. Khayet, C. Cojocaru, Air gap membrane distillation: desalination, modeling and optimization, Desalination 287 (2012) 138–145.
[134] A. Boubakri, A. Hafiane, S.A.T. Bouguecha, Application of response surface methodology for modeling and optimization of membrane distillation desalination process, J. Ind. Eng. Chem. 20 (5) (2014) 3163–3169.
[135] N. Kumar, A. Martin, Experimental modeling of an air-gap membrane distillation module and simulation of a solar thermal integrated system for water purification, Desalin. Water Treat. 84 (2017) 123–134.
[136] T. Mohammadi, P. Kazemi, M. Peydayesh, Optimization of vacuum membrane distillation parameters for water desalination using box-behnken design, Desalin. Water Treat. 56 (9) (2015) 2306–2315.
[137] A.A. Tashvigh, B. Nasernejad, Soft computing method for modeling and optimization of air and water gap membrane distillation—A genetic programming approach, Desalin. Water Treat. 76 (1) (2017) 30–39.
[138] H. Deng, et al., Modeling and optimization of solar thermal-photovoltaic vacuum membrane distillation system by response surface methodology, Sol. Energy 195 (2020) 230–238.
[139] H. Chang, J.-S. Liau, C.-D. Ho, W.-H. Wang, Simulation of membrane distillation modules for desalination by developing user's model on Aspen plus platform, Desalination 249 (1) (2009) 380–387.
[140] M. Khayet, C. Cojocaru, Artificial neural network modeling and optimization of desalination by air gap membrane distillation, Sep. Purif. Technol. 86 (2012/02/15/ 2012.) 171–182.
[141] M. Khayet, C. Cojocaru, Artificial neural network model for desalination by sweeping gas membrane distillation, Desalination 308 (2013/01/02/ 2013.) 102–110.
[142] F. Saffarimiandoab, R. Mattesini, W. Fu, E.E. Kuruoglu, X. Zhang, Insights on features' contribution to desalination dynamics and capacity of capacitive deionization through machine learning study, Desalination 515 (2021), 115197.
[143] N. AlSawaftah, W. Abuwatfa, N. Darwish, G. Husseini, A comprehensive review on membrane fouling: mathematical modelling, prediction, diagnosis, and mitigation, Water 13 (9) (2021) 1327.
[144] W. Guo, H.-H. Ngo, J. Li, A mini-review on membrane fouling, Bioresour. Technol. 122 (2012) 27–34.
[145] S. Park, S.-S. Baek, J. Pyo, Y. Pachepsky, J. Park, K.H. Cho, Deep neural networks for modeling fouling growth and flux decline during NF/RO membrane filtration, J. Membr. Sci. 587 (2019), 117164.
[146] I. Griffiths, A. Kumar, P. Stewart, A combined network model for membrane fouling, J. Colloid Interface Sci. 432 (2014) 10–18.
[147] Q.-F. Liu, S.-H. Kim, Evaluation of membrane fouling models based on bench-scale experiments: a comparison between constant flowrate blocking laws and artificial neural network (ANNs) model, J. Membr. Sci. 310 (1–2) (2008) 393–401.
[148] E.A. Roehl Jr., et al., Modeling fouling in a large RO system with artificial neural networks, J. Membr. Sci. 552 (2018) 95–106.
[149] B. De Jaegher, E. Larumbe, W. De Schepper, A. Verliefde, I. Nopens, Colloidal fouling in electrodialysis: a neural differential equations model, Sep. Purif. Technol. 249 (2020), 116939.

[150] M. Rezaei, D.M. Warsinger, M.C. Duke, T. Matsuura, W.M. Samhaber, Wetting phenomena in membrane distillation: mechanisms, reversal, and prevention, Water Res. 139 (2018) 329–352.
[151] B. Kim, Y. Choi, J. Choi, Y. Shin, S. Lee, Effect of surfactant on wetting due to fouling in membrane distillation membrane: application of response surface methodology (RSM) and artificial neural networks (ANN), Korean J. Chem. Eng. 37 (1) (2020) 1–10.
[152] P. Cabrera, J.A. Carta, J. González, G. Melián, Artificial neural networks applied to manage the variable operation of a simple seawater reverse osmosis plant, Desalination 416 (2017) 140–156.
[153] G. Zhang, et al., Data-driven optimal energy management for a wind-solar-diesel-battery-reverse osmosis hybrid energy system using a deep reinforcement learning approach, Energy Convers. Manag. 227 (2021), 113608.
[154] A.M. Gandhi, et al., Performance enhancement of stepped basin solar still based on OSELM with traversal tree for higher energy adaptive control, Desalination 502 (2021), 114926.
[155] R. Porrazzo, A. Cipollina, M. Galluzzo, G. Micale, A neural network-based optimizing control system for a seawater-desalination solar-powered membrane distillation unit, Comput. Chem. Eng. 54 (2013) 79–96.
[156] S. Madaeni, M. Shiri, A. Kurdian, Modeling, optimization, and control of reverse osmosis water treatment in kazeroon power plant using neural network, Chem. Eng. Commun. 202 (1) (2015) 6–14.
[157] S. Tayyebi, M. Alishiri, The control of MSF desalination plants based on inverse model control by neural network, Desalination 333 (1) (2014) 92–100.
[158] S. Vafakhah, Z. Beiramzadeh, M. Saeedikhani, H.Y. Yang, A review on free-standing electrodes for energy-effective desalination: recent advances and perspectives in capacitive deionization, Desalination 493 (2020), 114662.